AD-A039 323 NAVAL POSTGRADUATE SCHOOL MONTEREY CALIF F/G 17/1
DEVELOPMENT OF A FLEXURAL DISK TRANSDUCER FOR ACOUSTIC TRACKING--ETC(U)
DEC 76 O SEVDIK

UNCLASSIFIED NL

| OF |
AD
A039323

END

DATE
FILMED
5-77

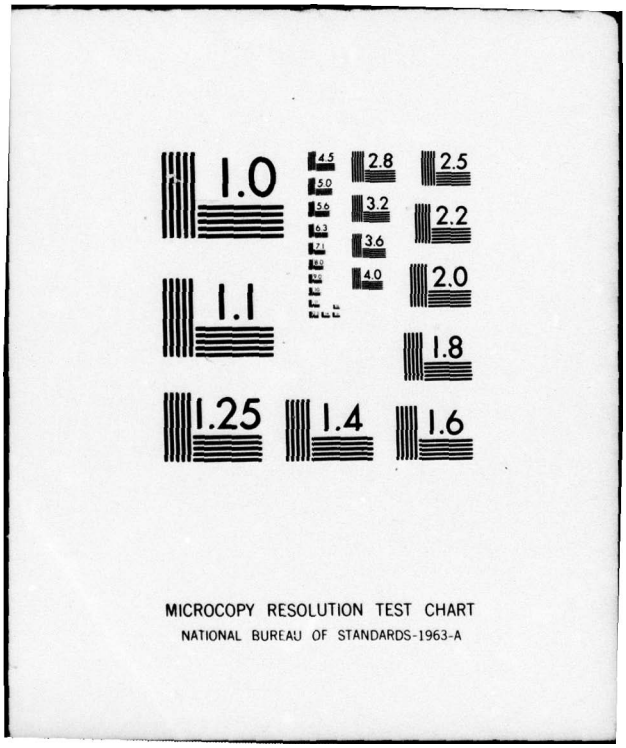
1.0
1.1
1.25
1.4
1.6
1.8
2.0
2.2
2.5
2.8
3.2
3.6
4.0
4.5
5.0
5.6
MICROCOPY RESOLUTION TEST CHART
NATIONAL BUREAU OF STANDARDS-1963-A

(1)

NAVAL POSTGRADUATE SCHOOL

Monterey, California

THESIS

DEVELOPMENT OF A FLEXURAL DISK TRANSDUCER FOR ACOUSTIC TRACKING OF UNDERWATER VEHICLES

by

Omer SEVDIK

December 1976

Thesis Advisor: O. B. Wilson

Approved for public release; distribution unlimited.

Unclassified

SECURITY CLASSIFICATION OF THIS PAGE (When Data Entered)

REPORT DOCUMENTATION PAGE	READ INSTRUCTIONS BEFORE COMPLETING FORM
1. REPORT NUMBER	2. GOVT ACCESSION NO. / 3. RECIPIENT'S CATALOG NUMBER
4. TITLE (and Subtitle) (6) Development of a Flexural Disk Transducer for Acoustic Tracking of Underwater Vehicles.	(9) 5. TYPE OF REPORT & PERIOD COVERED Master's Thesis; December 1976 / 6. PERFORMING ORG. REPORT NUMBER
7. AUTHOR(s) (10) Omer SEVDIK	8. CONTRACT OR GRANT NUMBER(s)
9. PERFORMING ORGANIZATION NAME AND ADDRESS NAVAL POSTGRADUATE SCHOOL Monterey, California 93940	10. PROGRAM ELEMENT, PROJECT, TASK AREA & WORK UNIT NUMBERS
11. CONTROLLING OFFICE NAME AND ADDRESS NAVAL POSTGRADUATE SCHOOL Monterey, California 93940	(11) 12. REPORT DATE Dec [redacted] 76 / 13. NUMBER OF PAGES (12) 68p.
14. MONITORING AGENCY NAME & ADDRESS(if different from Controlling Office) NAVAL POSTGRADUATE SCHOOL Monterey, California 93940	15. SECURITY CLASS. (of this report) Unclassified / 15a. DECLASSIFICATION/DOWNGRADING SCHEDULE

16. DISTRIBUTION STATEMENT (of this Report)

Approved for public release; distribution unlimited.

17. DISTRIBUTION STATEMENT (of the abstract entered in Block 20, if different from Report)

18. SUPPLEMENTARY NOTES

19. KEY WORDS (Continue on reverse side if necessary and identify by block number)

Flexural Disk Transducer

20. ABSTRACT (Continue on reverse side if necessary and identify by block number)

A high frequency, broad-band transducer which has a broad radiation pattern in a half space is required for acoustic tracking of underwater vehicles. Two models of a flexural disk transducer, were built and tested. It was found that the radiation loading in water completely damps the resonances due to standing flexural waves and the radiation appears to be due entirely to flexural waves propagating in the disk. Broad-band

over

DD FORM 1 JAN 73 1473 (Page 1) EDITION OF 1 NOV 65 IS OBSOLETE S/N 0102-014-6601

Unclassified

SECURITY CLASSIFICATION OF THIS PAGE (When Data Entered)

251450

radiation patterns and broad bandwidth (60-80 kHz) were obtained.The discrepancies between theory and experiment are attributed in part to violation of the thin plate assumptions and to lack of knowledge of the actual velocity distributions. This approach offers promise for achieving the desired broad beam widths.However,additional development work is needed to obtain a transducer which has the curved face necessary for smooth hydrodynamic flow.

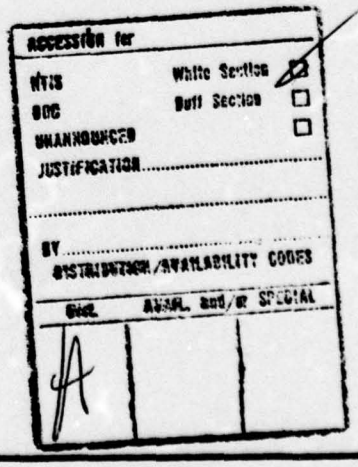

DEVELOPMENT OF A FLEXURAL DISK TRANSDUCER FOR ACOUSTIC TRACKING OF UNDERWATER VEHICLES

by

Omer SEVDIK
Lieutenant, Turkish Navy
B.Sc.E.A., Naval Postgraduate School, 1976

Submitted in partial fulfillment of the
requirements for the degree of

MASTER OF SCIENCE IN ENGINEERING ACOUSTICS

from the
NAVAL POSTGRADUATE SCHOOL
December 1976

Author: Omer Sevdik

Approved by: O B Wilson, Jr.
Thesis Advisor

D A Stevens
Second Reader

H E Walker
Chairman, Department of Physics and Chemistry

Robert R Fossum
Dean of Science and Engineering

ABSTRACT

A high frequency, broad-band transducer which has a broad radiation pattern in a half space is required for acoustic tracking of underwater vehicles. Two models of a flexural disk transducer, were built and tested. It was found that the radiation loading in water completely damps the resonances due to standing flexural waves and the radiation appears to be due entirely to flexural waves propagating in the disk. Broad-band radiation patterns and broad bandwidth (60-80 kHz) were obtained. The discrepancies between theory and experiment are attributed in part to violation of the thin plate assumptions and to lack of knowledge of the actual velocity distributions. This approach offers promise for achieving the desired broad beam widths. However, additional development work is needed to obtain a transducer which has the curved face necessary for smooth hydrodynamic flow.

TABLE OF CONTENTS

LIST OF FIGURES

ACKNOWLEDGEMENTS

I am fortunate to have this opportunity to thank the people who have helped in the preparation of this thesis.First of all I am most indebted to my advisor,Professor O.B.Wilson,for his guidance and motivation.Also,I wish to express my sincere appreciation to Lieutenant Commander,V.Auns and Lieutenant A.Ford for their assistance in preparation of this thesis and Mr.R.Moeller for his assistance in constructing the transducers.

I wish to acknowledge the unfailing support and tolerance of my wife,Bahar.

I want to thank the Turkish and United States Navies for creating this generous opportunity.

Last but not least I should also like to thank the Naval Torpedo Station Keyport,Washington for their technical and financial support.

I. INTRODUCTION

For observing the position of submerged targets on underwater ranges, target-mounted sound sources are commonly used with fixed, bottom-mounted arrays. In order to insonify a large volume of water, essentially non-directicnal sources are required.

Considering the geometry of one tracking range,that at the Naval Torpedo Station(NTS),Keyport, Washington, which has a typical vertical distance of 200 m and the distance between bottom-mounted hydrophone arrays of about 2000 meters, the maximum slant range,r, can be found to be 1020 m. Using the following formula for transmission loss (TL), the transmission loss at the range,r, can be calculated:

$$TL = 20 \text{ Log } r + a.r$$

For a sound frequency of 75 kHz, the attenuation coefficient, a, for sea water is about 0.03 dB per meter. The transmission losses are 91 and 52 dB at ranges of 1020 and 200 m,respectively; hence, directional properties of the target-mounted sound source must compensate for this 40 dB difference in TL. Consideration of the pitch and roll motions of the underwater vehicle and the effect of the reflection from the surface has led to the specification that the scurce radiate uniformly within a conical volume 150 degrees wide, centered on the vertical axis of the transducer.

The practical shape of the beam pattern is shown in Fig 1 has been calculated considering the difference in transmission loss with angle.

In order to obtain the necessary source level at 75 degrees from the main axis, it is required to drive the transducer at large amplitudes.This however, apparently has shortened transducer life(From informal communication with NTS); accordingly redistribution of total energy away from main axis was a major design consideration. It is felt that this would extend the Mean Time Between Failure(MTBF) of the transducer and associated amplifiers.

Sufficient bandwidth for pulse code modulated telemetry and economy cf the construction were additional goals.

Formerly, this requirement was met by a pop-out transducer,utilizing a spherical piezoelectric ceramic element.However,for current high-speed targets the performance of the protruding radiator is unsatisfactory,due principally to fluid flow problems. Therefore,a number of designs of flush mount transducers have been built and used for this purpose.

One approach to obtaining a broad beam radiation pattern is the use of a two element concentric piston transducer with amplitude and phase shading has been studied and which appears to offer promise (Ref. 4).Another approach is that of Mr. M.Barlow,at the Naval Torpedo Station, who proposed the idea of and carried out some initial experiments using flexural waves in a small disk for this purpose(private communication).

The intent of this study has been to explore further the use of transverse (flexural) vibrations in a plate as an approach in the development of a flush-mount transducer

capable of generating broad beam patterns at high frequencies.

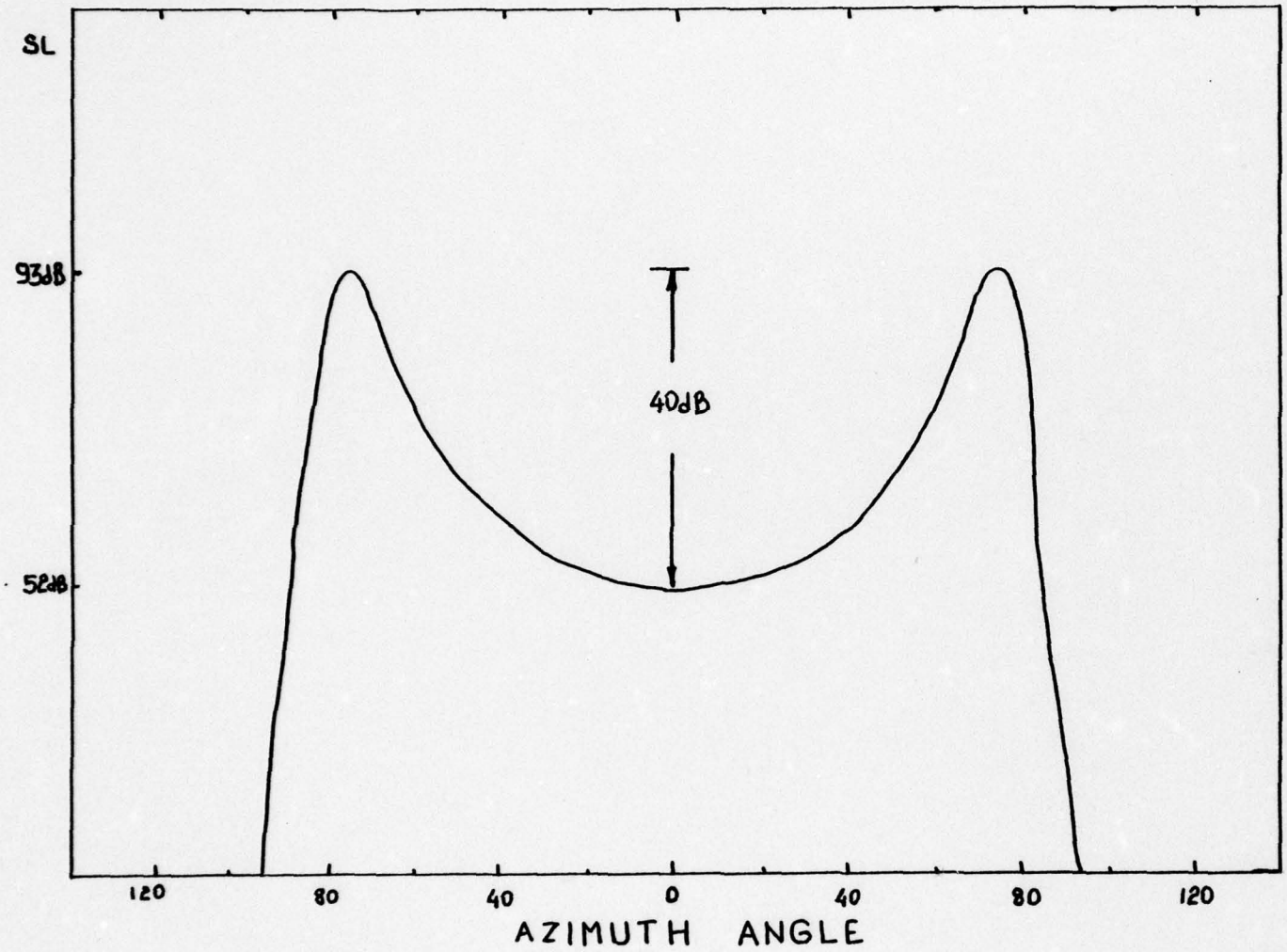

Figure 1 - PRACTICAL RADIATION PATTERN

II. THEORETICAL CONSIDERATIONS

The derivation of the transverse wave equation for thin plates is given in texts on theory of elasticity (Ref. 1 p. 214). The equation is,

$$\nabla^4 w + \frac{3\rho(1-s^2)}{Q\,h^2} \cdot \frac{\partial^2 w}{\partial t^2} = 0 \qquad 2.1$$

where w is the displacement in the transverse direction, ρ is the density of the material, s is the Poisson's ratio, Q is the modulus of elasticity (Young's Modulus) and h is the half thickness of the plate. It has been assumed that h is small compared to the transverse wave length.

For simple harmonic motion of a plate,

$$w = Y(r,\phi)\ e^{-i2\pi ft}$$

and a differential equation for Y can be written:

$$(\nabla^2 - \gamma^2)(\nabla^2 + \gamma^2) Y = 0$$

where

$$\gamma = \frac{12\pi^2 f^2 \rho(1-s^2)}{Q\,h^2}$$

The solution of the first equation in polar coordinates, which is finite at r = 0, is,

$$Y = \begin{matrix}\text{Cos}\\ \text{Sin}\end{matrix} (m\phi) \quad J_m(\gamma r)$$

where m is an integer. The solution of the second equation is obtained from the first equation by changing γ into $i\gamma$ .It is called the Hyperbolic Bessel Function and is defined as

$$I_m(z) = i^{-m} \quad J_m(iz) \quad .$$

Possible solutions for the simple harmonic oscillations of a plate are therefore given by the following expression:

$$Y(r,\phi) = \begin{matrix}\text{Cos}\\ \text{Sin}\end{matrix} (m\phi) \left[A\ J_m(\gamma r) + B\ I_m(\gamma r) \right] \quad .$$

A and B are derived from boundary conditions.

The boundary conditions for a circular plate of radius a,clamped its edges are:

$$Y(a,\phi) = 0 \quad \text{and} \quad \frac{\partial Y}{\partial r} = 0 \quad \text{at } r=a.$$

The first condition is satisfied by making

$$B = - A \frac{J_m(\gamma a)}{I_m(\gamma a)}$$

and the second condition is satisfied by requiring γ to satisfy

$$I_m(\gamma a)\frac{\partial}{\partial r}J_m(\gamma r) - J_m(\gamma a)\frac{\partial}{\partial r}I_m(\gamma r) = 0 \quad \text{at} \quad r=a.$$

Because $\gamma = \gamma(f)$, this equation fixes the allowed frequencies.

One can label the solutions for this second condition:

$$\gamma_{mn} = \left(\frac{\pi}{a}\right)\beta_{mn}$$

where

$$\beta_{01} = 1.015 \qquad \beta_{02} = 2.007 \qquad \beta_{03} = 3.000$$

A more complete tabulation of values of β_{mn} is given in Ref. 1, p. 215.

The allowed frequencies for the normal modes are;

$$f_{mn} = \frac{\pi h}{2a^2}\left[\frac{a}{3\rho(1-\sigma^2)}\right]^{1/2}(\beta_{mn})^2 \qquad 2.2$$

and the characteristic functions are:

$$\psi = \begin{matrix}\cos\\ \sin\end{matrix}(m\phi)\left[J_m\left(\frac{\pi r\beta_{mn}}{a}\right) - \frac{J_m(\pi\beta_{mn})}{I_m(\pi\beta_{mn})}I_m\left(\frac{\pi r\beta_{mn}}{a}\right)\right]$$

On the other hand, the transverse wave speed c_b for plate without losses is given at Ref 2,p. 508,

$$c_b = \omega^{1/2}\left(\frac{B}{M}\right)^{1/4}$$

where $$B = \frac{Q(2h)^3}{12(1-s^2)}$$

is the stiffness of the plate for bending and M is the mass of the plate per unit surface.

The following expression gives the value of the plate half thickness:

$$h = \frac{c_b^2}{2\pi f\left[\frac{Q}{3\rho(1-s^2)}\right]^{1/2}} \qquad 2.3$$

Hence, for a given frequency and plate material one can find a direct relationship between the thickness of the plate and the transverse wave speed c_b from equation 2.3.One can also find a relationship between the radius a and thickness 2h by using equation 2.2.In combining these two results the relationship between radius and thickness can be obtained.

For aluminum plates (Ref 3)

$\rho = 2700 \text{ kg/m}^3$

$Q=7.1 \quad 10^{10}$ nt / m^2

$s=.33$

For the (0,2) mode,and a frequency of 75 KHz

$a^2 = 0.2627\ h$

$c_b^2 = 1.47 \quad 10^9\ h$

Computation of the radiation pattern function was based on a variation of a program worked out by Shaw (Ref 4).In this case, the radiation pattern is the sum of radiations from a set of 20 concentric ring piston elements.An assumption is made about the amplitude and phase of the velocity of motion as a function of piston radius.

The pattern for any ring,say number n, which has outer and inner radii of a_n and a_{n-1} respectively and a velocity amplitude U_n, is computed by subtracting the ordinary,uniform piston radiation pattern function of radius a_{n-1} with velocity amplitude U_n from that of a piston of radius a_n and velocity U_n.

A computer program shown in Appendix A was used to estimate the radiation patterns for combinations of various modes and radii.

None of the patterns so obtained were found to resemble the specifications described before in the introduction section,but only (0,2) mode offered some promise. One of the calculated radiation pattern is shown in Fig 2.

Also,radiation from circular progressive wave was estimated using the computer program given in Appendix B.

The equation for the displacement of an outgoing circular progressive flexural wave is:

$$w = A \; H_o^{(2)} (k_b r)$$

where $H_o^{(2)}$ =Hankel function of the second kind

Using the same method described above radiation patterns of various thickness and radius combinations were obtained.One of them is shown in Fig 3.

III. EXPERIMENTAL PROCEDURES

Based on the theoretical beam patterns,a plate with half thickness, h=1.5 mm and a radius r=2.38 cm, was chosen for a first try and the transducer shown in Fig 4 was constructed.Some dimensions were specified by the positioning and mounting hole for the transducer on the extender section of the test vehicle.

To drive this transducer,a hollow piezo-ceramic cylinder, with radial polarization which has following specifications was used :

Ceramic:GLENNITE HS21

Length: 1.0 in

Outer diameter: 0.5 in

Wall thickness : 0.125 in

Longitudinal resonance: 89.63 kHz

Using a compcsite transducer configuration with mass-loading on the ends due to two pieces of aluminum(Fig 5), the longitudinal resonance was reduced to 73.6 kHz. In order to attach the masses to the element a nut and bolt were used;however, for driving the plate the nut was found to be unnecessary.Without it, it was assumed that the longitudinal resonance would approach 75 kHz.

Upon completion of the construction, electrical

admittance measurements of the transducer were made using a Dranetz Impedance-Admittance meter.The result for the unloaded transducer(in air) is shown in Fig 6.Primary resonances were found at frequencies:

66.34 kHz, 73.26 kHz, 80.4 kHz, 105.2 kHz.

The configuration shown in (Fig 7) and a Capacitive Displacement Probe (Ref 4 Fig 35) which averages displacement over the probe face were used to determine the modes of vibration for each resonance. After careful (and difficult) measurements the amplitude distribution of 66.34 kHz was found to resemble closely that expected for the (0,2) mode.The distribution at 73.26 kHz resembled somewhat that expected for the (0,3) mode.However the pattern was not symmetrical.It is believed that this is one of the mixed-modes. Relative amplitude distributions are shown in Figs 8-10.

Next the transducer was placed in the extender section.In this instance, admittance measurements showed small deviations from earlier resonance frequencies; however, when the mounted transducer was placed into water,none of the earlier resonances were found,except for the one at 72.27 kHz. Both admittance curves appear in Fig 11.It appears that the radiation loading completely damps the normal modes of flexural vibration of the plate and that the resonance at 72.27 kHz is associated with the longitudinal vibration of the ceramic driver element.

Measurements of the radiation pattern of the transducer were made in one of the Naval Postgraduate School's anechoic water tanks using apparatus described below. The transducer was mounted in the wall of an aluminum cylinder which was the extender section of a 12-3/4 inches diameter torpedo.

The transducer baffle assembly can be rotated about a vertical axis.A potentiometer mounted on a shaft in the drive train provides an electrical signal which is proportional to angle of rotation which can be used to drive one axis of a graphical plotter.

In order to eliminate the effects of surface reflections,and minimize the effects of standing waves in the tank the pulse mode of operation was used.In this mode,the Boxcar Integrator, gated to the direct path pulse, generates a d.c voltage proportional to the amplitude of the pulse.This voltage is fed to a calibrated logarithmic converter which then generates the ordinate of the beam pattern in decibels.To improve signal to noise ratio(SNR), a high driving voltage (30 vrms or more) was used.The transducer and hydrophone were located with a two meter separation. The following test equipment was connected as shown in Fig 12:

Hewlett Packard 7035 B X-y Recorder

Tektronix RM45A Dual Trace Oscilloscope

Hewlett Packard 465A Voltage Amplifier

PAR 160 Boxcar Integrator

Krohn-Hite DCA 50R Power Amplifier

Harrison 6205 B D.C. Power Supply

40 dB. Gate

General Radio 1396A Tone Burst Generator

General Radio 1192B Frequency Counter

Hewlett Packard 204C Oscillator

Hewlett Packard 407A Power Amplifier

LC-10 Hydrophone

Envelope Detector

Hewlett Packard 7561A Logarithmic Converter

The radiation pattern for various frequencies are presented in Figs 13-21.

It is believed that the measured radiation patterns are due principally to the progressive transverse wave in the plate and not, as first theorized, to the existance of standing flexural waves in the plate.

The results show that radiation patterns below 60 kHz do approach the pattern which is shown earlier in Fig 1. However above 60 kHz, the level along the axis increases relative to that at larger angles. The broad beam width characteristics appear to change little with frequency.

A second transducer was built with a thicker plate (4 mm) which should result in a larger transverse wave speed.

Driving this new model (MOD 2) with the same ceramic element, the admittance curves shown in Figs 21-23 were obtained. The results were almost the same as earlier model. In water, the resonance was found at 72.24 kHz.

Using the same configuration of test instruments shown in Fig 12, reasonably good radiation patterns were obtained below 78 kHz for this new model (Figs 24-29).

In an attempt to understand better the details of motion of the vibrating plate when in water, near field pressure measurements were made using the following equipment:

Hewlett Packard 204C Oscillator

General Radio Frequency Counter

Hewlett Packard 467A Power Amplifier

Krohn Hite DCA 50R Power Amplifier

Tektronix RM45A Oscilloscope

LC-5 Hydrophone

Dranetz Phasemeter 305

Hewlett Packard 403B Voltmeter

The LC-5 hydrophone was placed about 1 or 2 mm from the face of the transducer in the anechoic tank. A rack and pinion assembly supporting the hydrophone permitted moving the hydrophone across the face of the transducer for near field measurements. Continuous excitation was used. The figures obtained for near field pressure amplitudes and phases are presented in Fig 30 and 31 for the MOD 1 transducer, and in Figs 32 and 33 for the MOD 2 transducer when driven at the resonance frequency. Another measurement made at 60 kHz driving frequency gave the results shown in Figs 34-35.

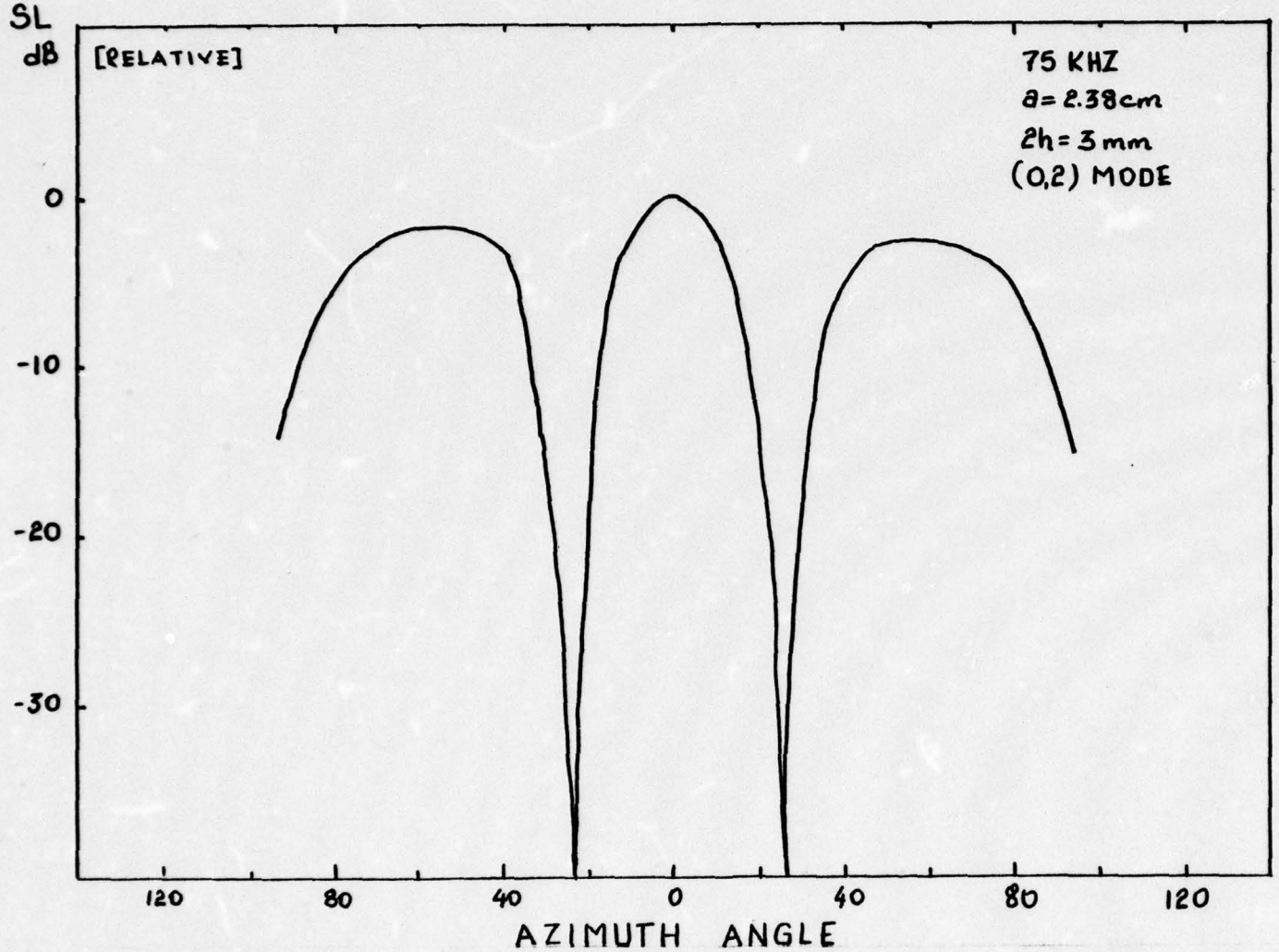

Figure 2 - CALCULATED RADIATION PATTERN USING NORMAL MODE SOLUTION

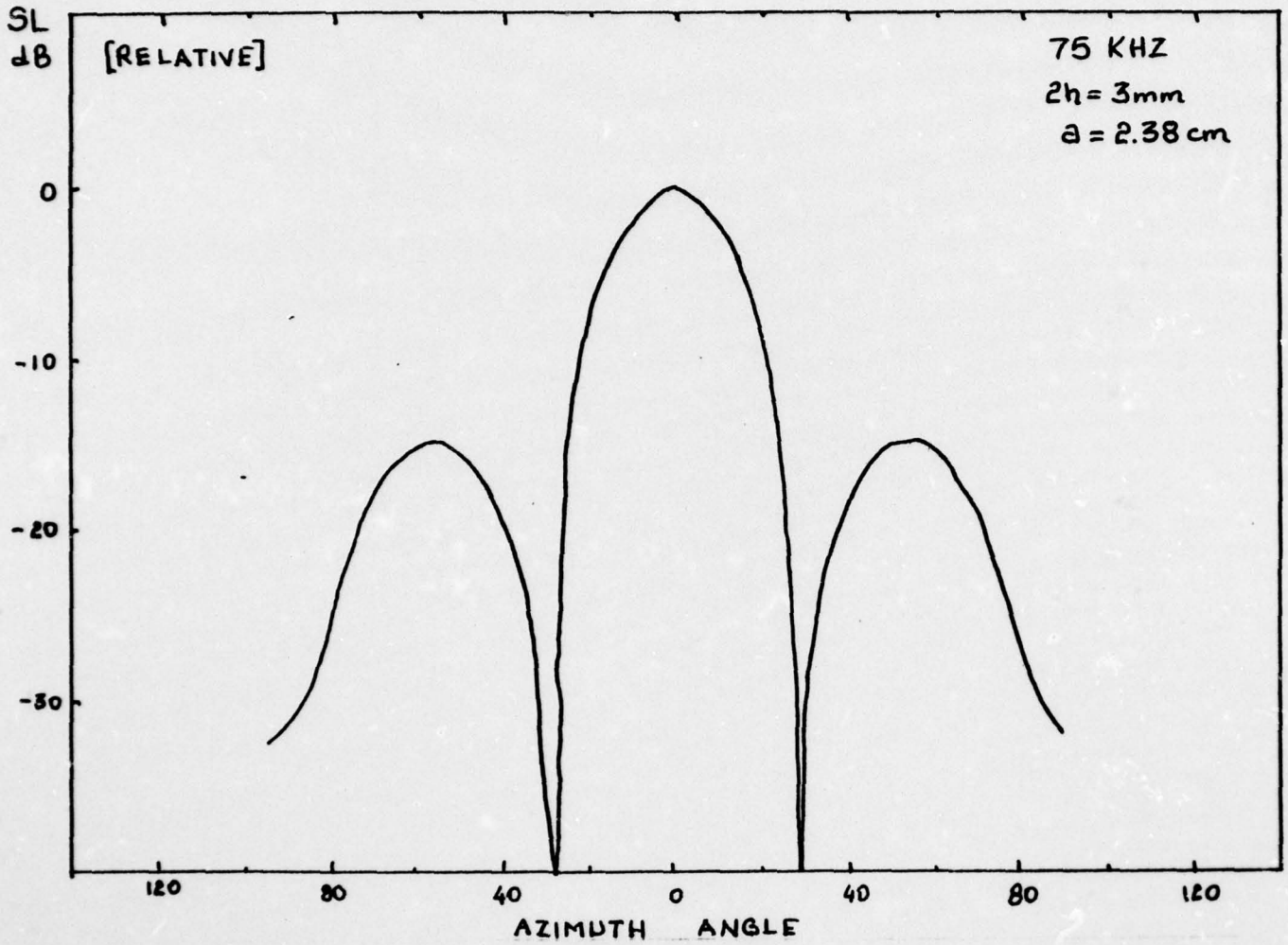

Figure 3 - CALCULATED RADIATION PATTERN USING PROGRESSIVE WAVE SOLUTION

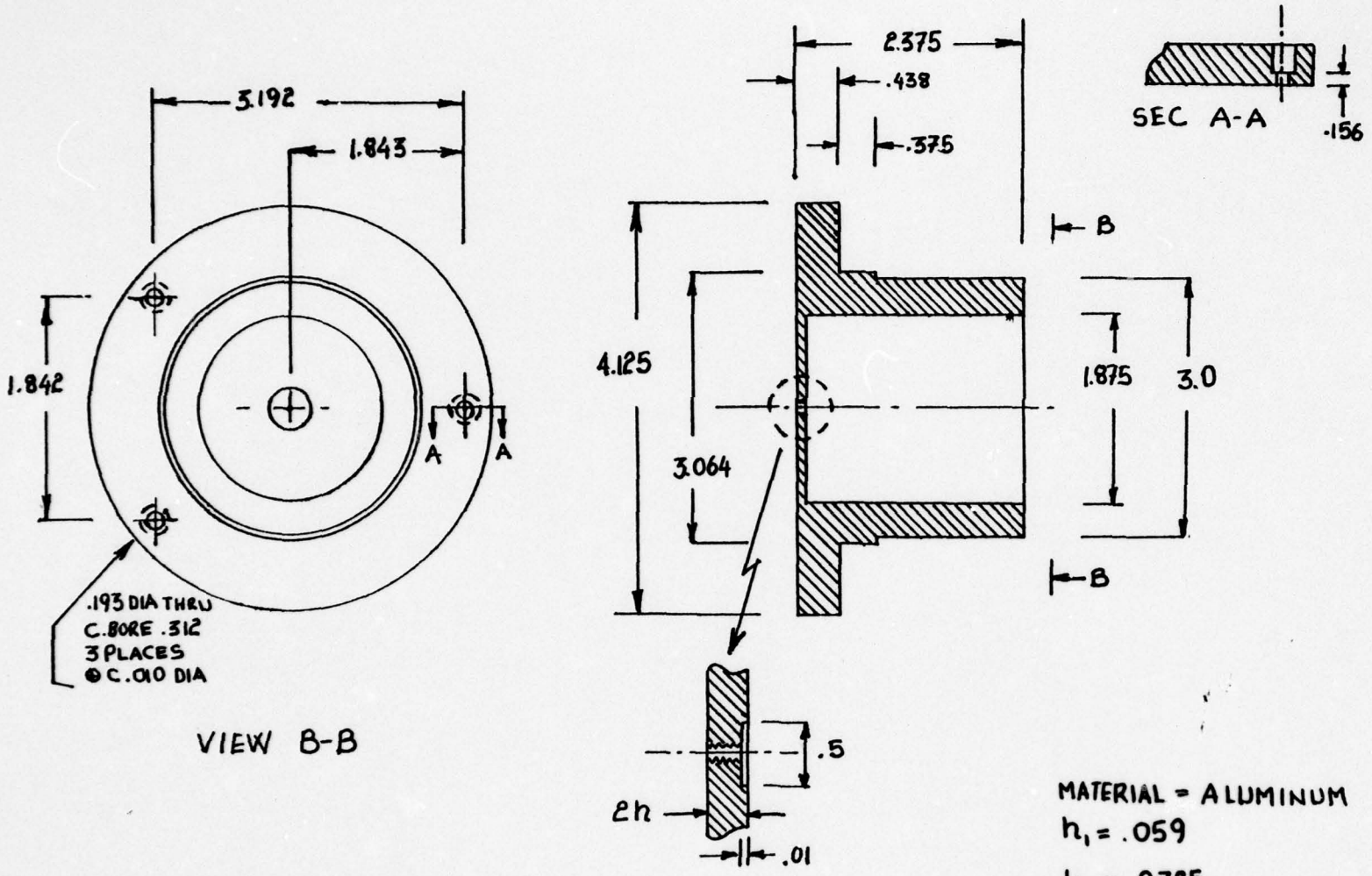

Figure 4 - TRANSDUCER DIMENSIONS

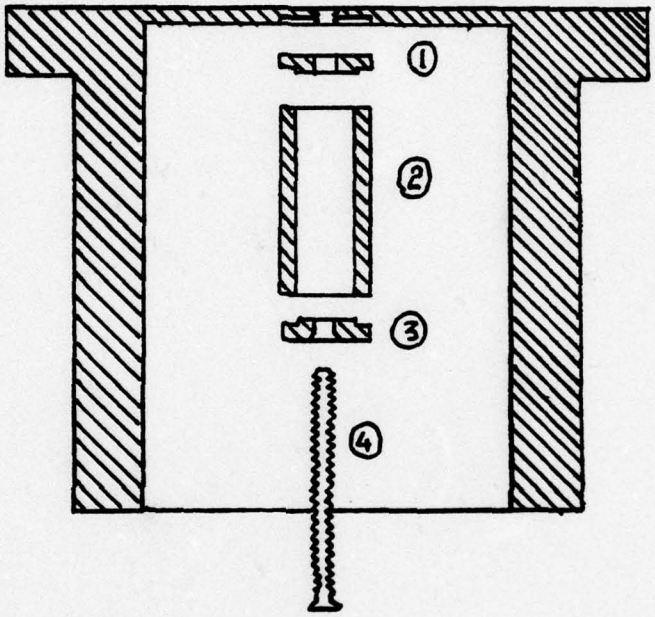

① AND ③ : ALUMINUM MASSES

② : CERAMIC ELEMENT

④ : SCREW

Figure 5 - TRANSDUCER AND DRIVING ELEMENT

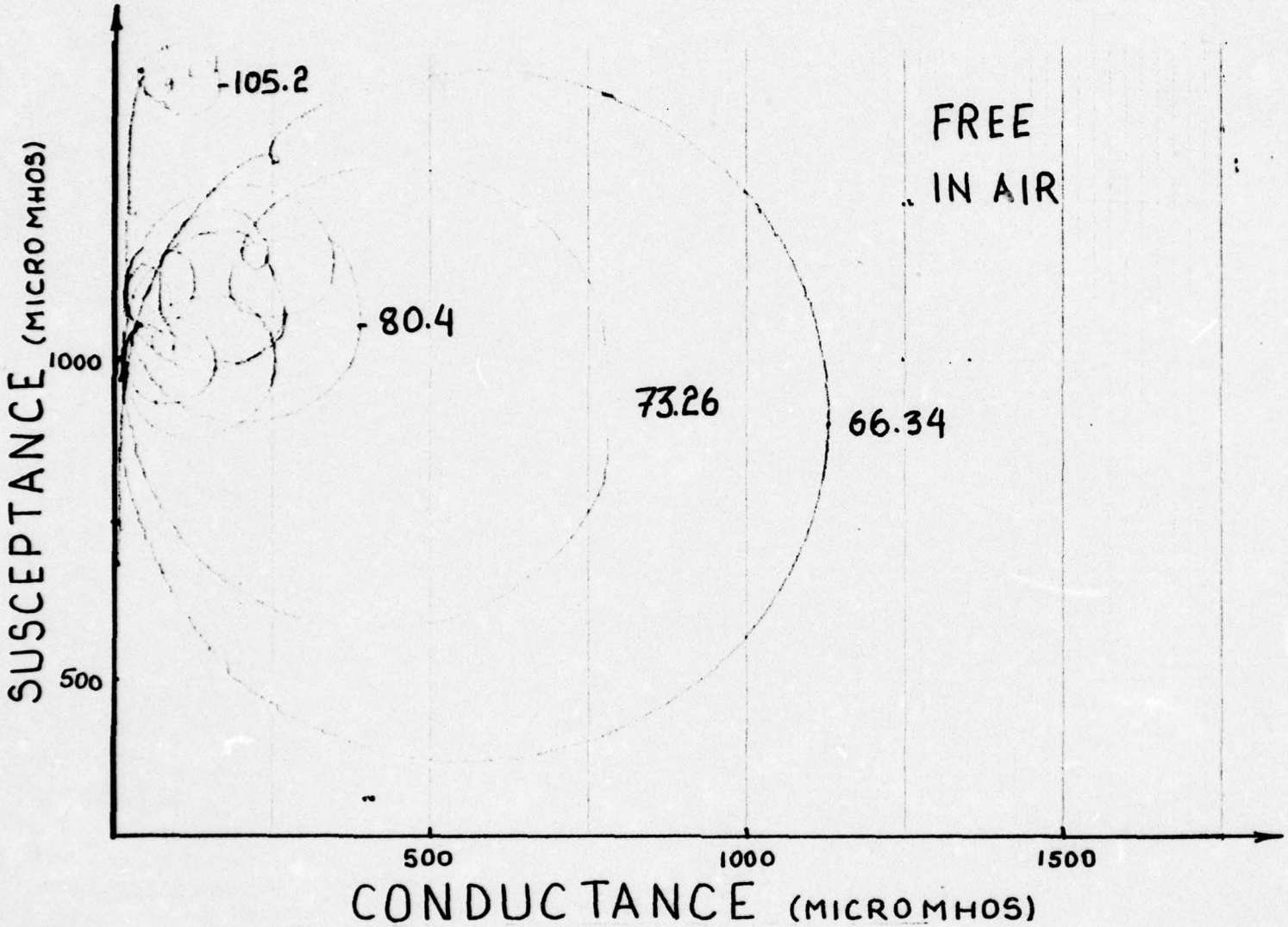

Figure 6 - ADMITTANCE IN AIR

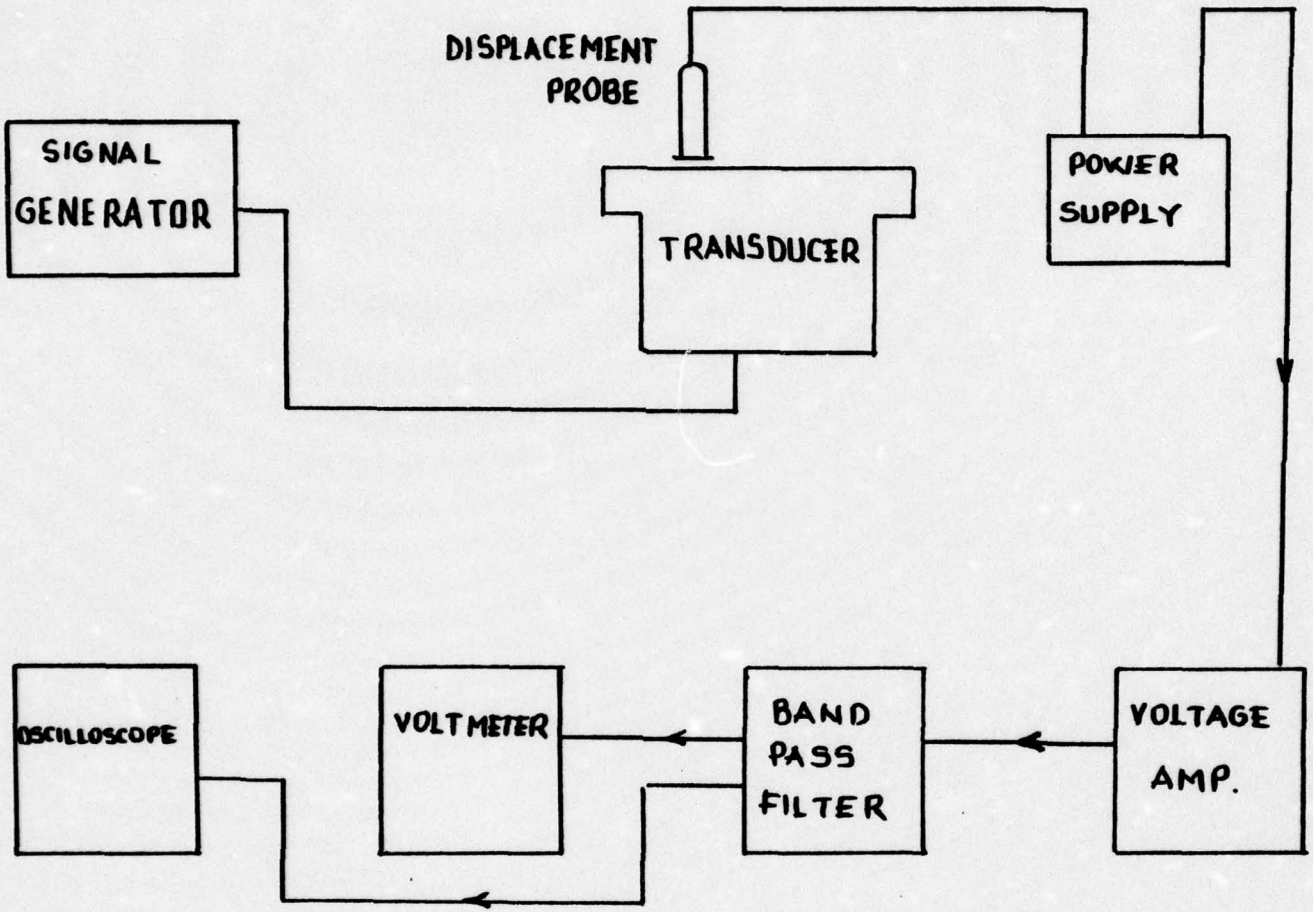

Figure 7 - DISPLACEMENT MEASUREMENTS

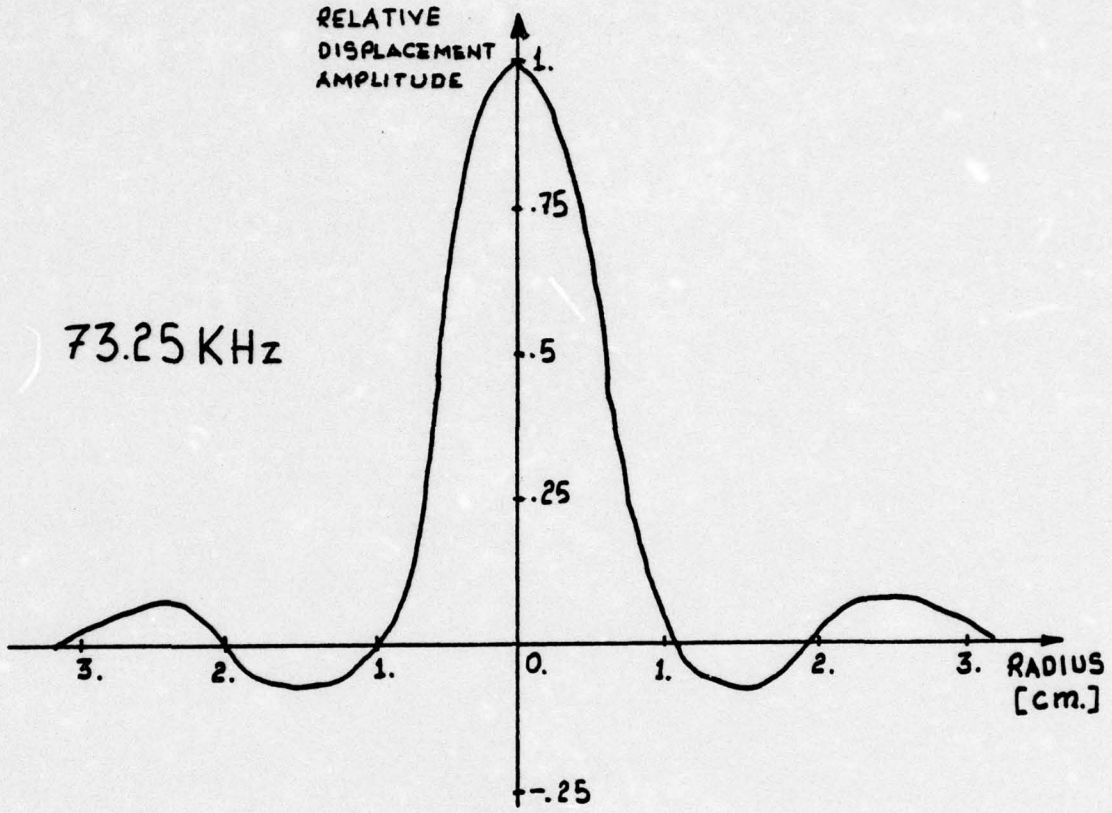

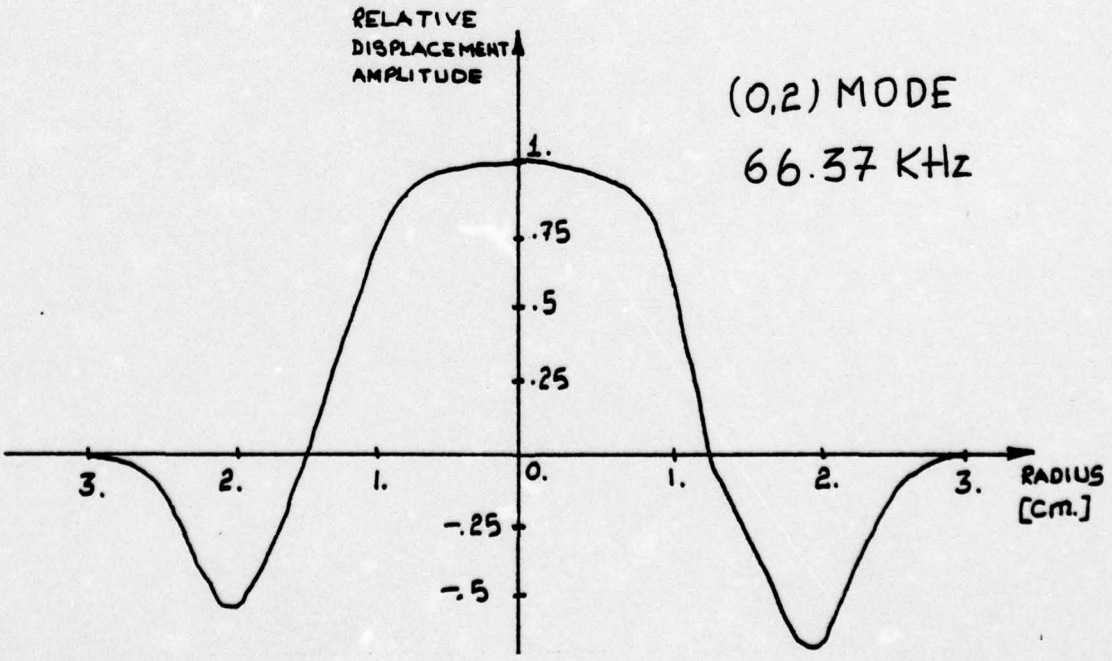

Figure 8 - RELATIVE DISPLACEMENT AMPLITUDES

(0.2) MODE AMPLITUDE DISTRIBUTION
66.37 KHz.

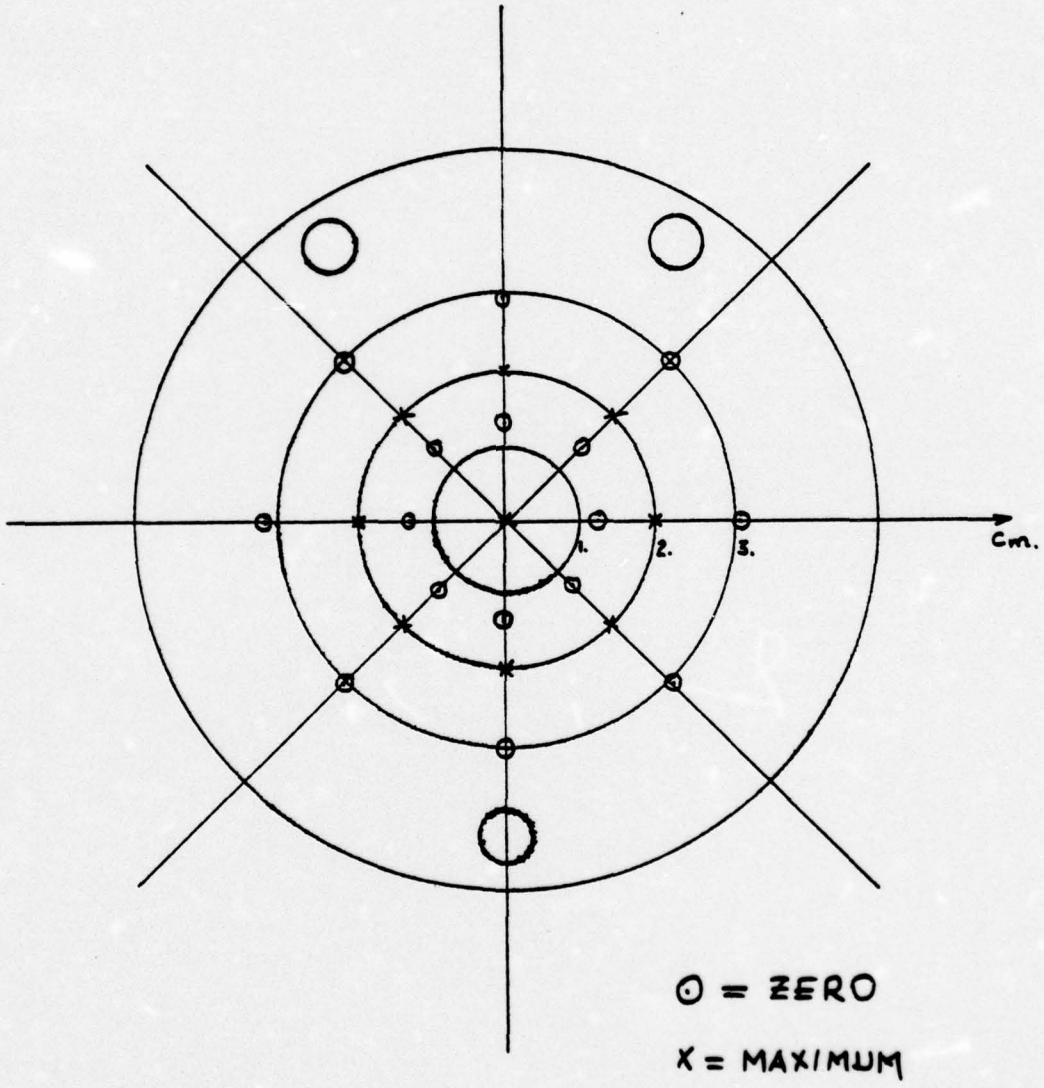

Figure 9 - AMPLITUDE DISTRIBUTION ON THE FACE OF THE TRANDUCER

AMPLITUDE DISTRIBUTION

73.24 KHz.

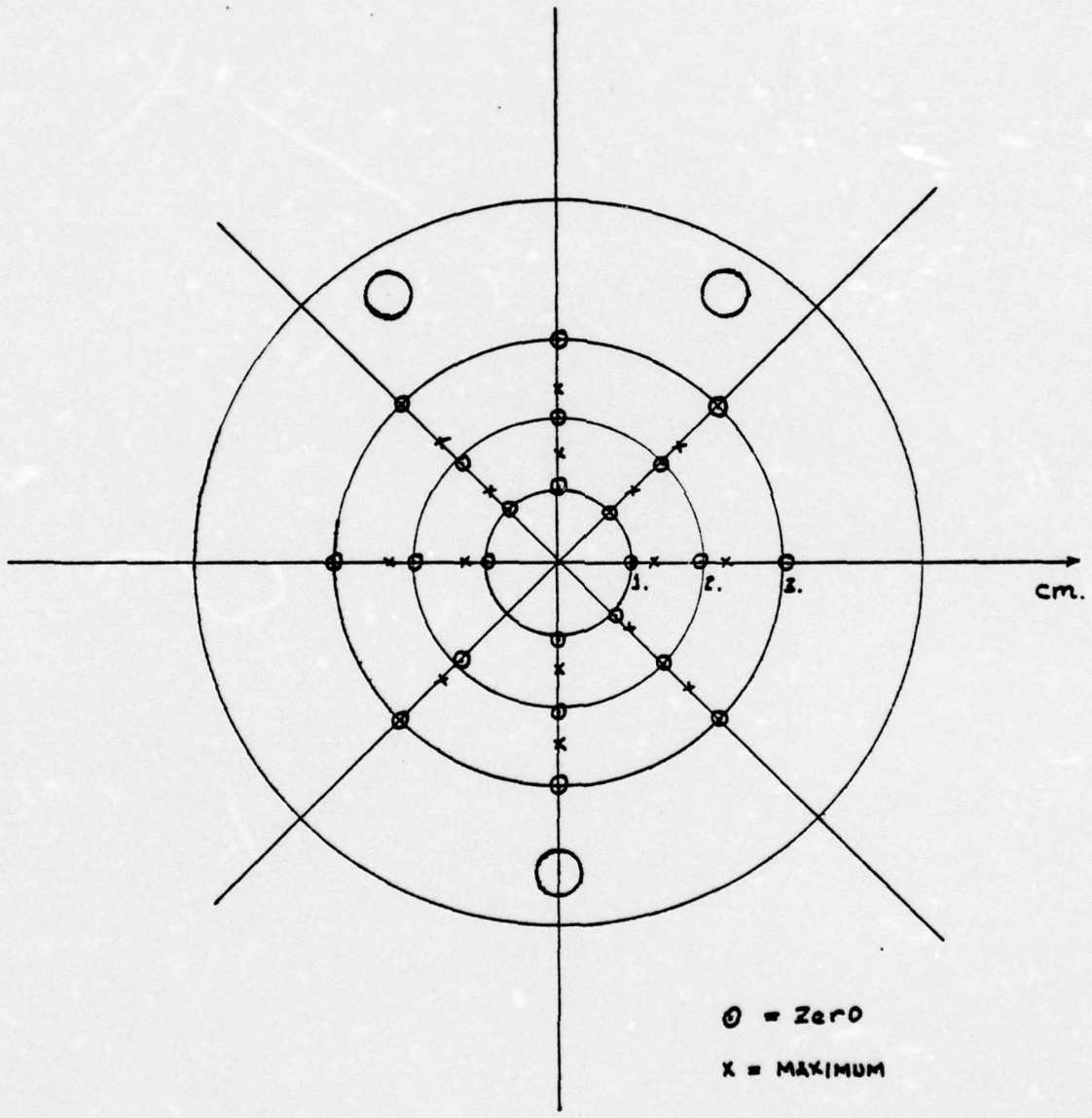

Figure 10 - AMPLITUDE DISTRIBUTION ON THE FACE OF THE TRANDUCER

Figure 11 - ADMITTANCE MEASUREMENTS MOUNTED IN EXTENDER SECTION IN AIR

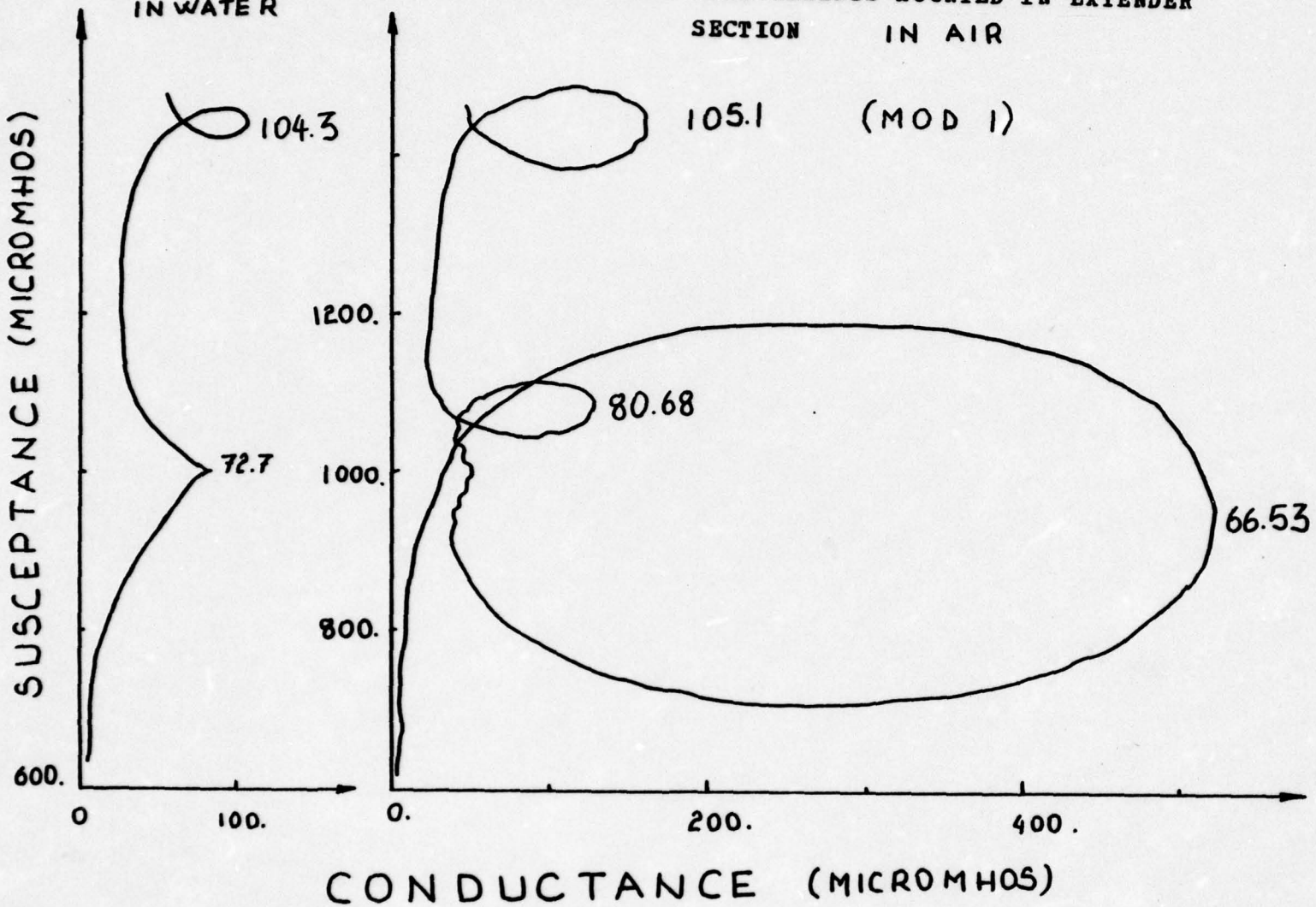

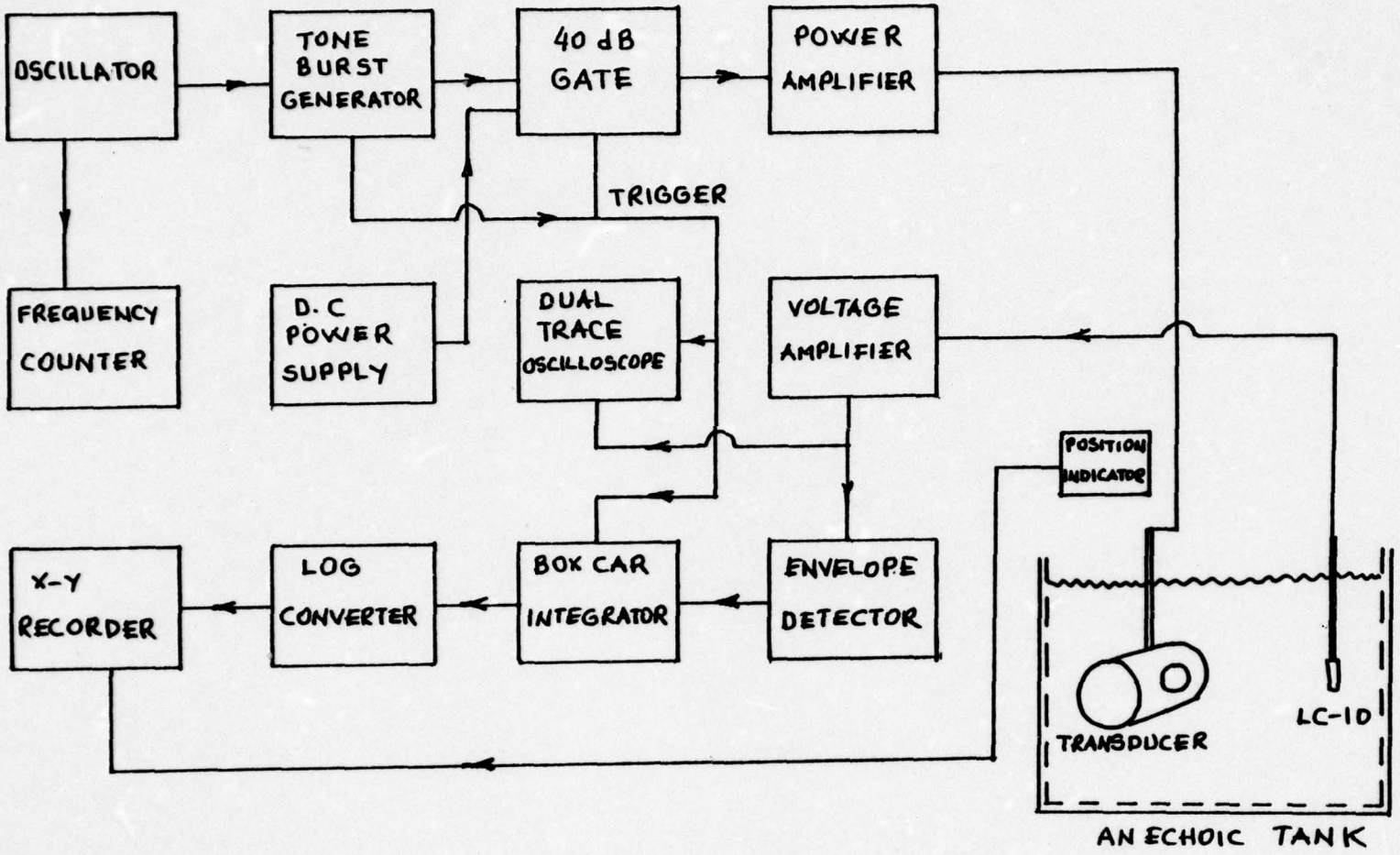

Figure 12 - APPARATUS FOR BEAM PATTERN MEASUREMENTS

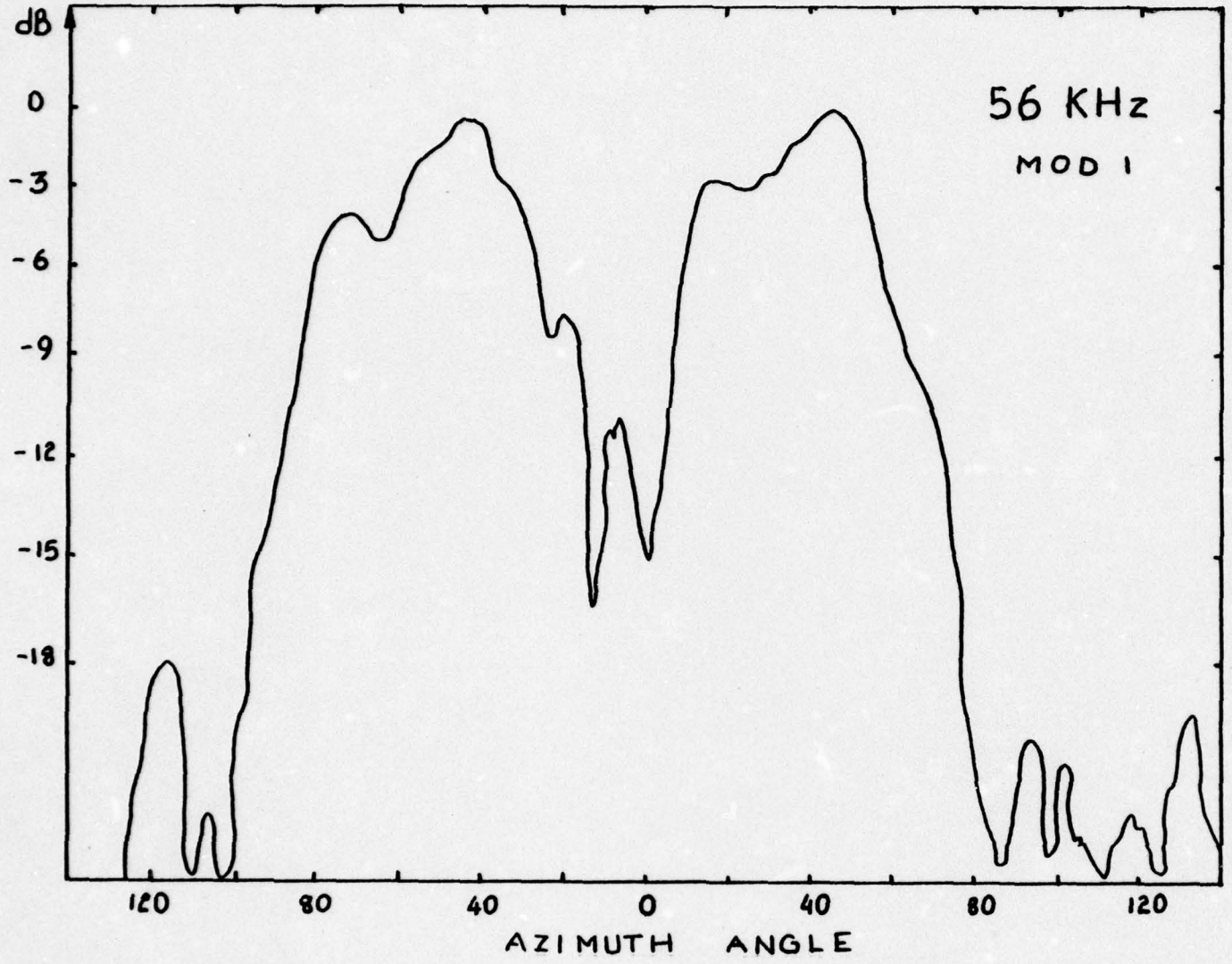

Figure 13 - RADIATION PATTERN

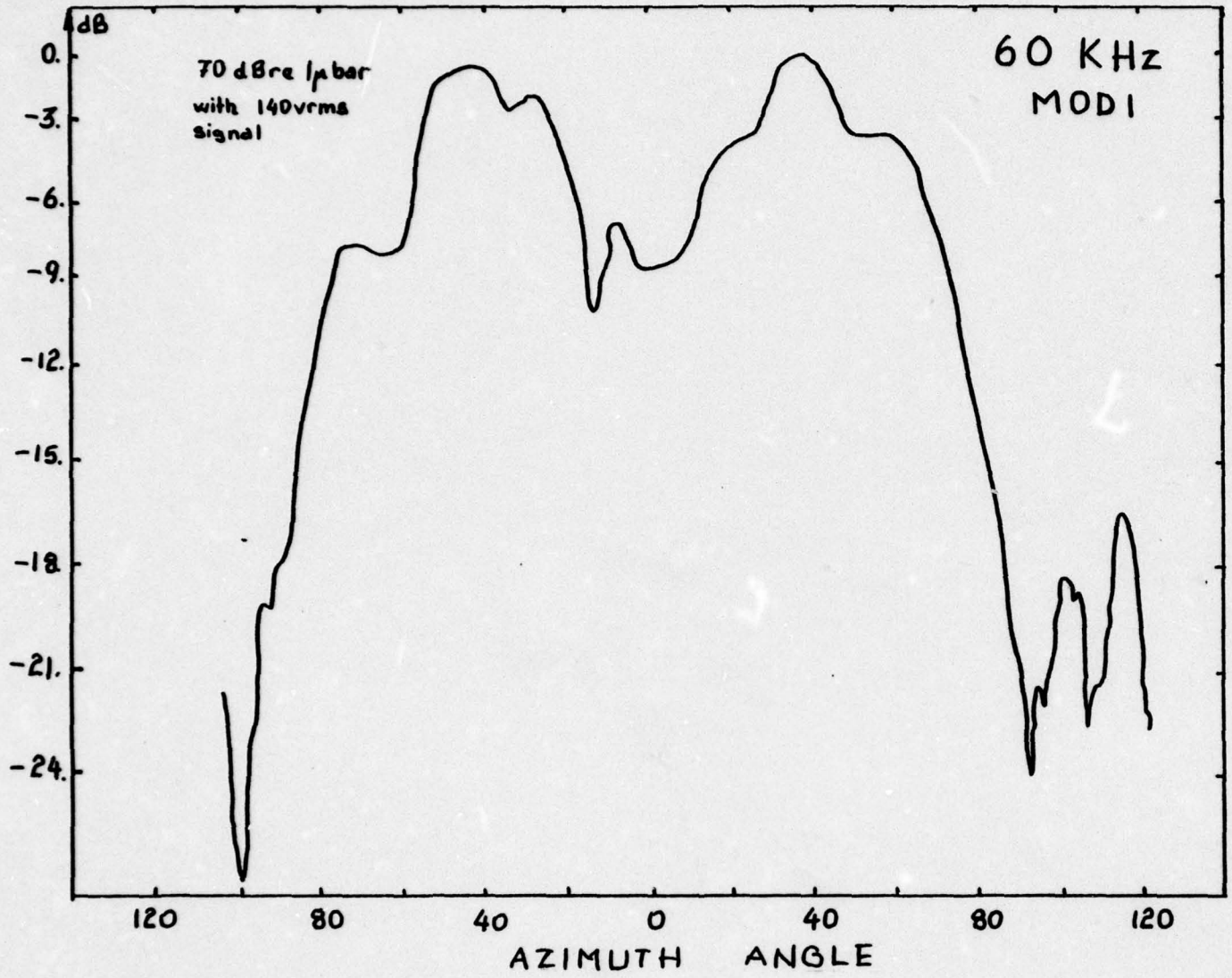

Figure 14 - RADIATION PATTERN

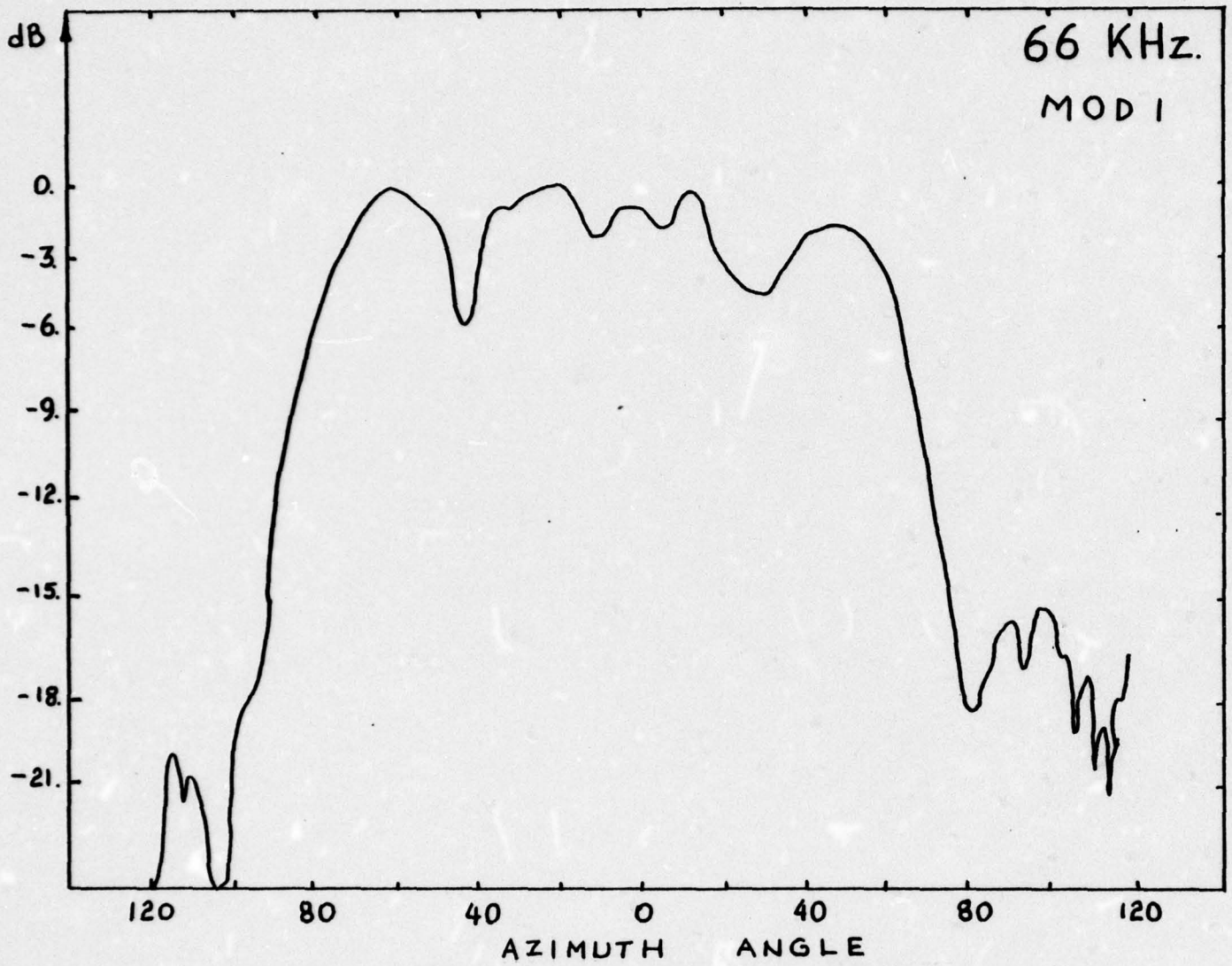

Figure 15 - RADIATION PATTERN

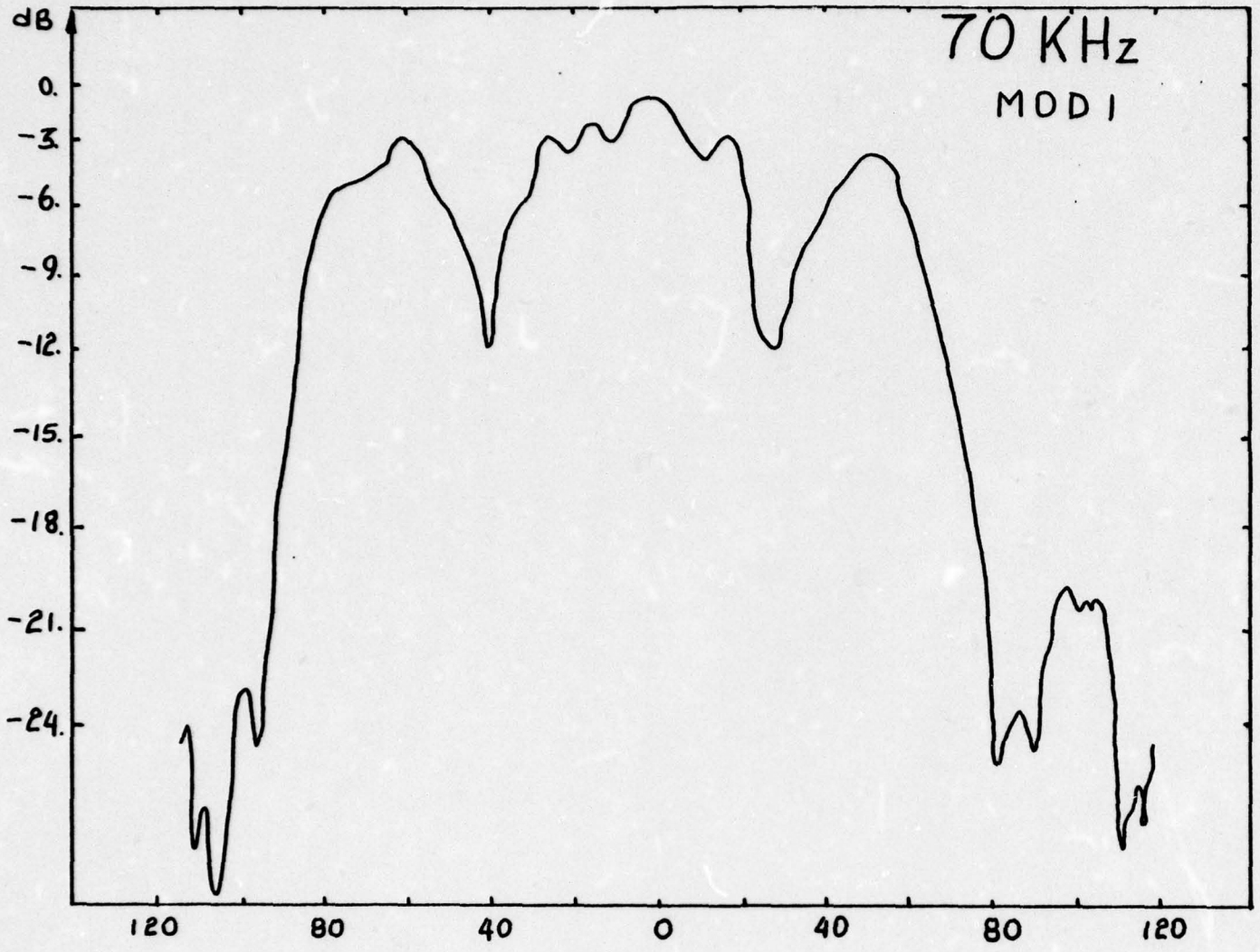

Figure 16 - RADIATION PATTERN

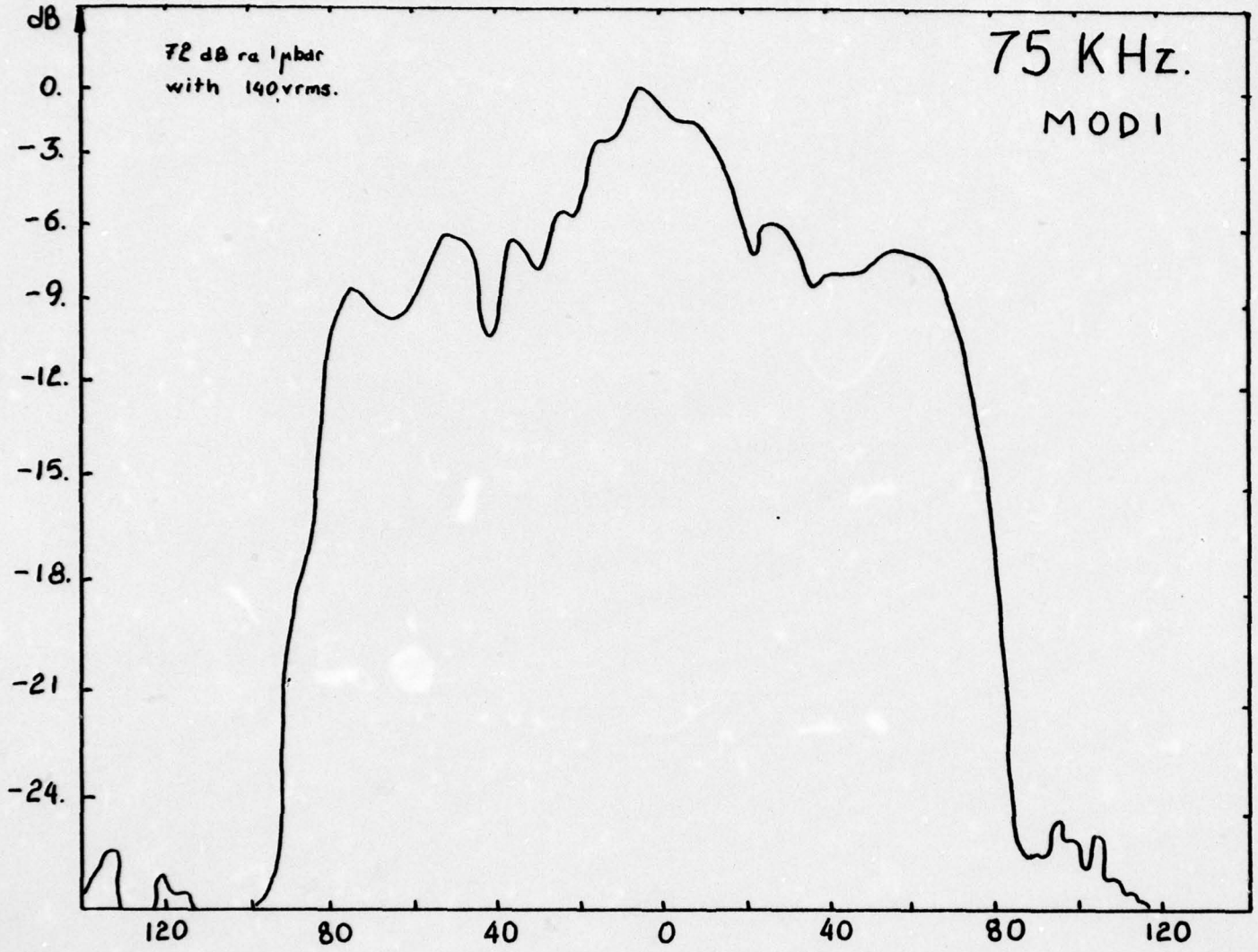

Figure 17 - RADIATION PATTERN

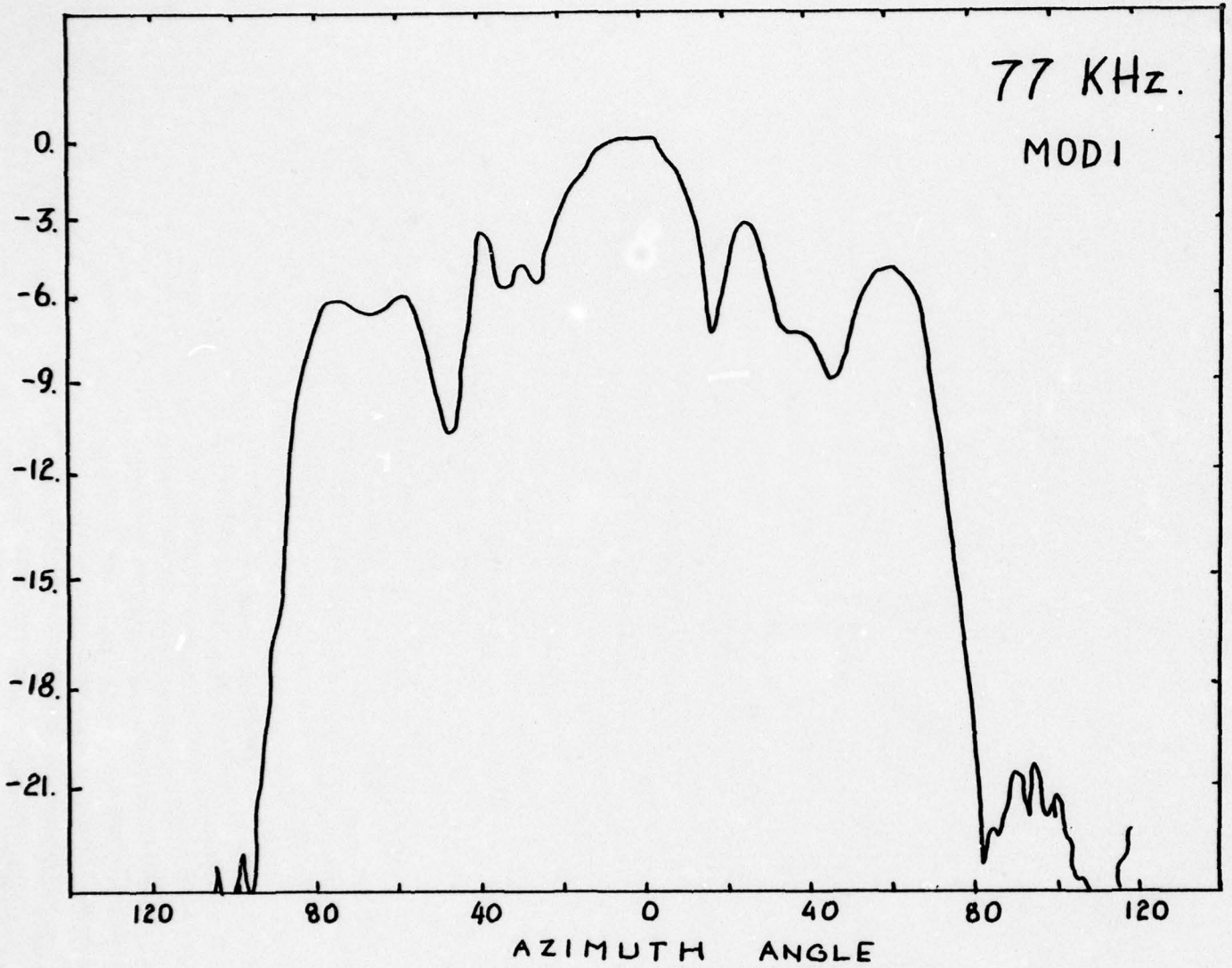

Figure 18 - RADIATION PATTERN

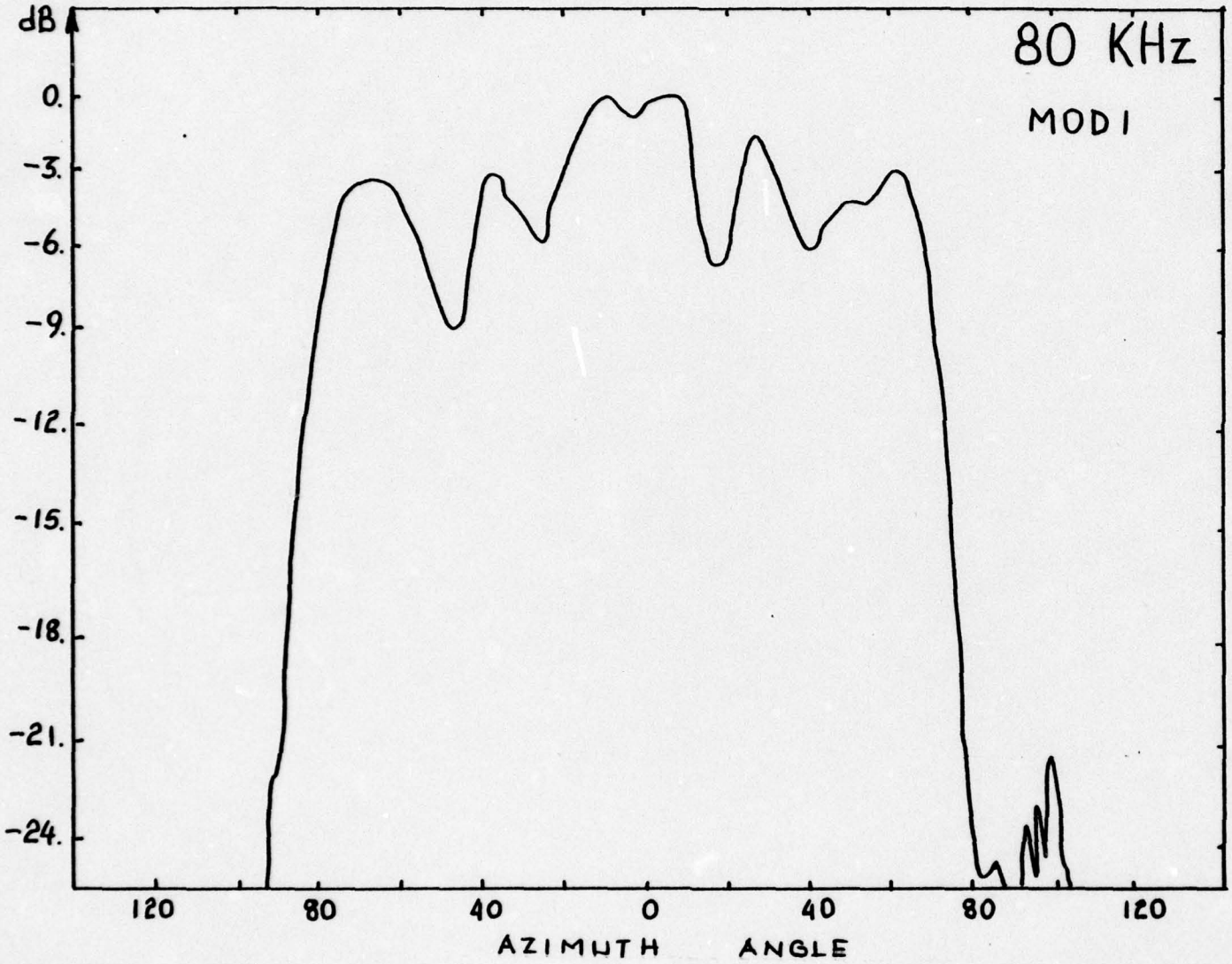

Figure 19 - RADIATION PATTERN

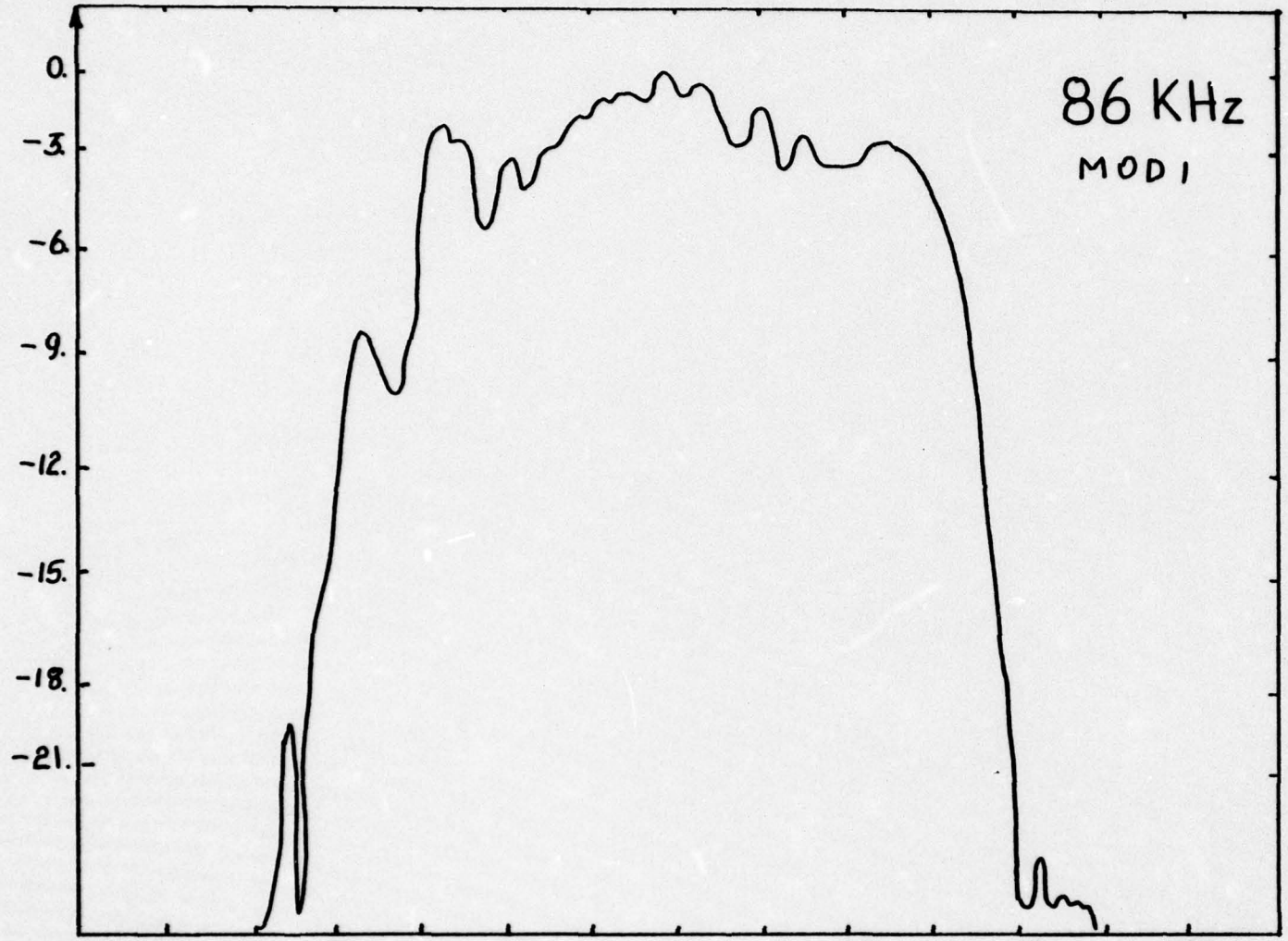

Figure 20 - RADIATION PATTERN

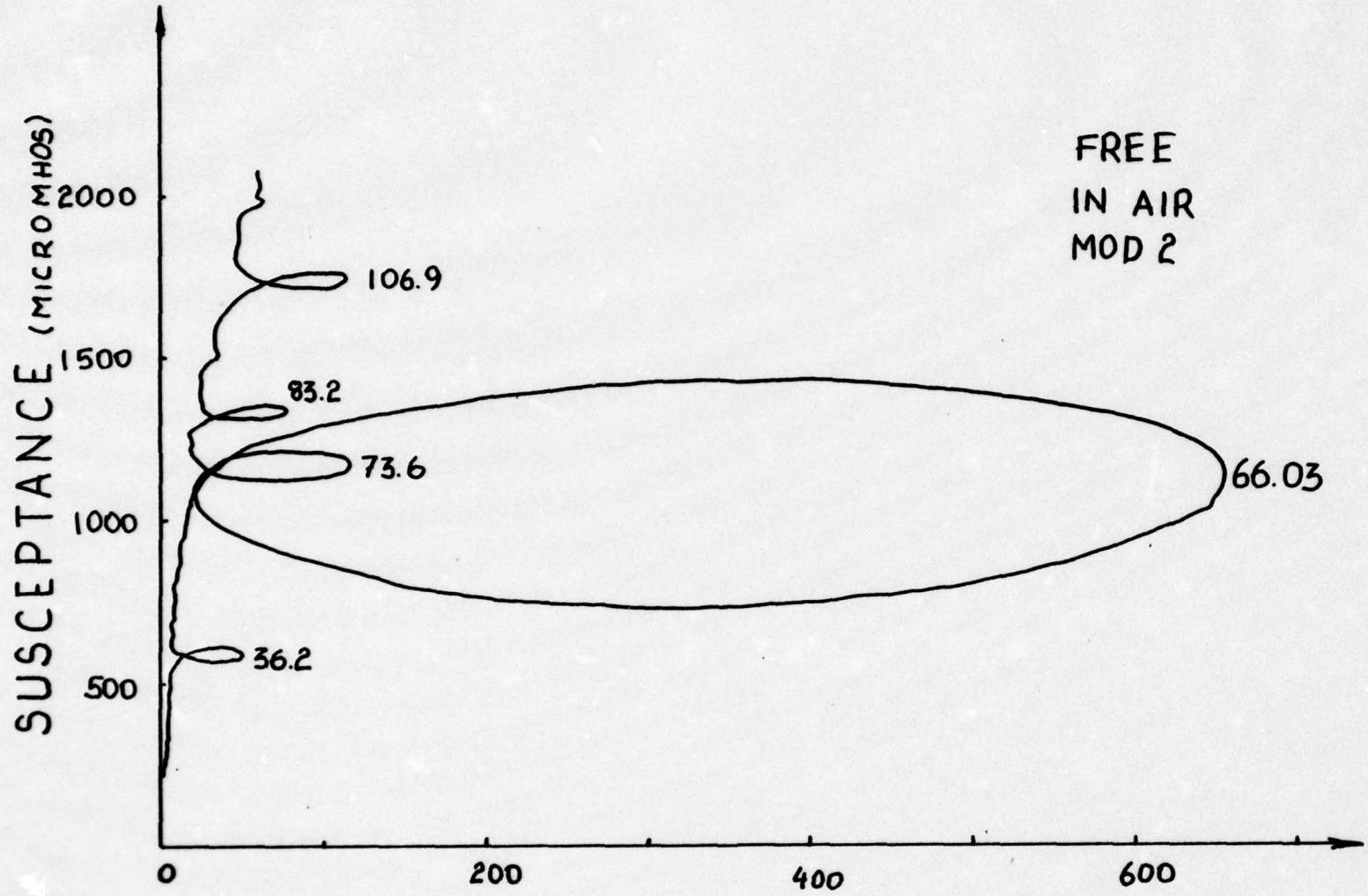

Figure 21 - ADMITTANCE MEASUREMENT

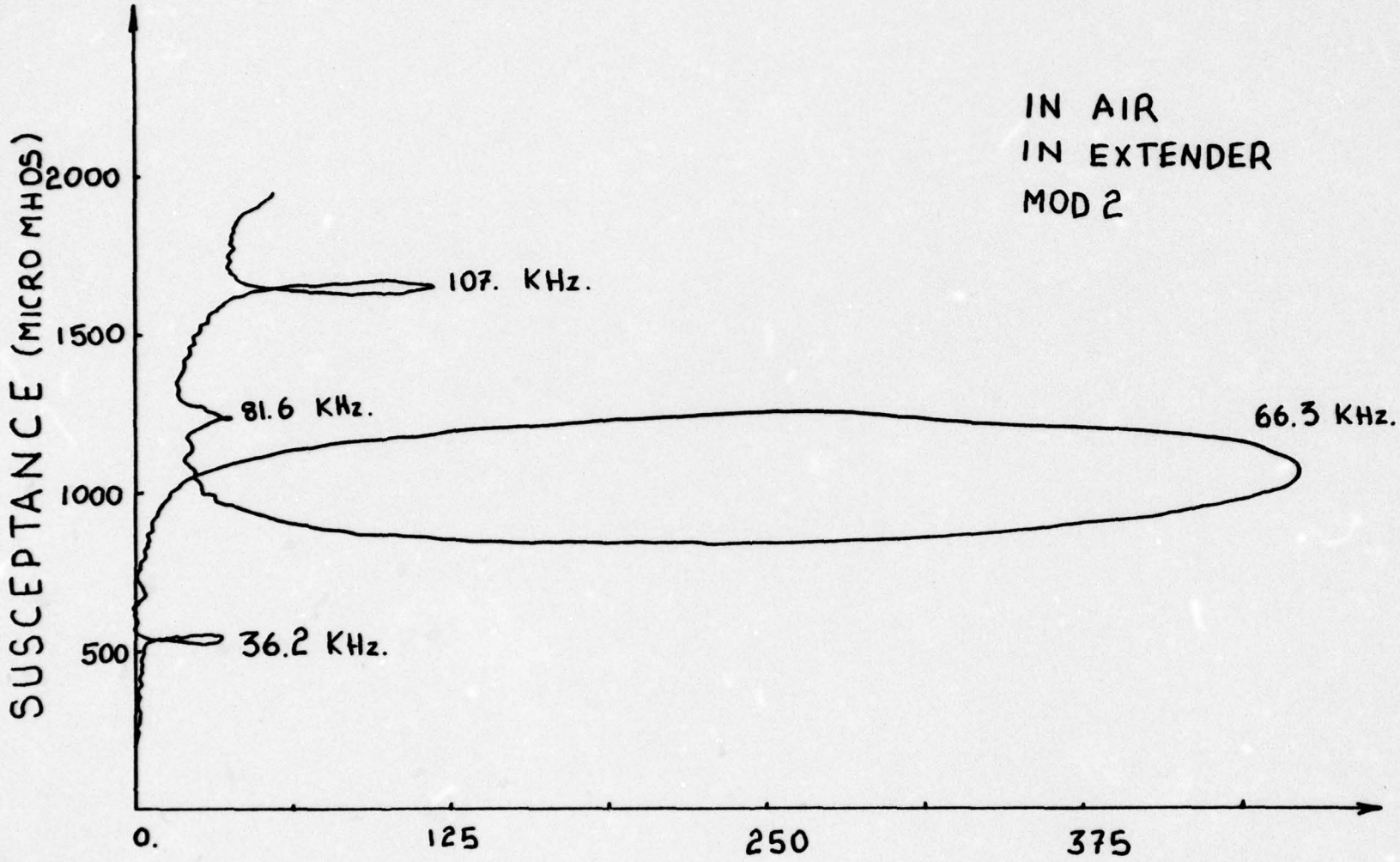

Figure 22 - ADMITTANCE MEASUREMENT

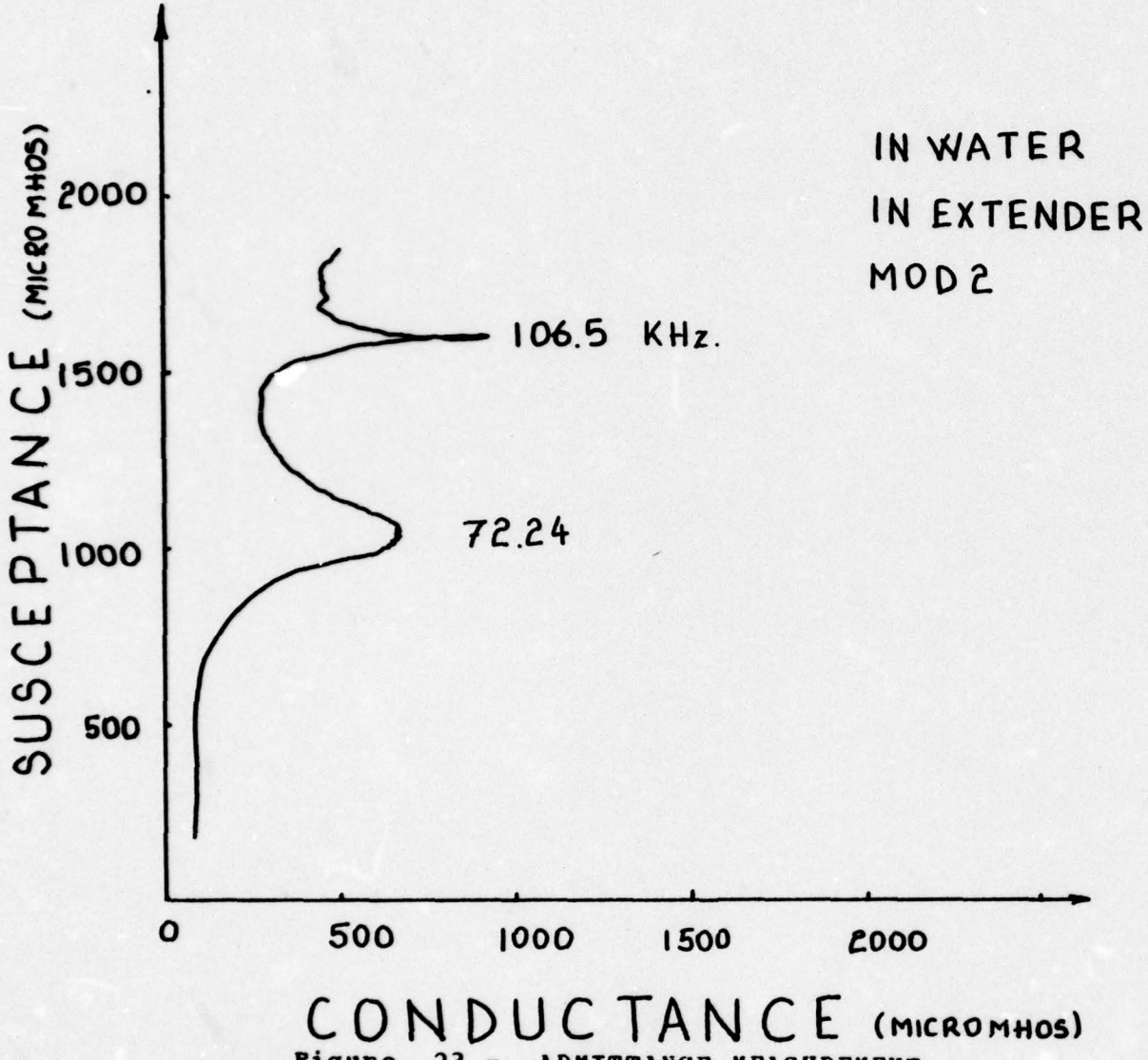

Figure 23 - ADMITTANCE MEASUREMENT

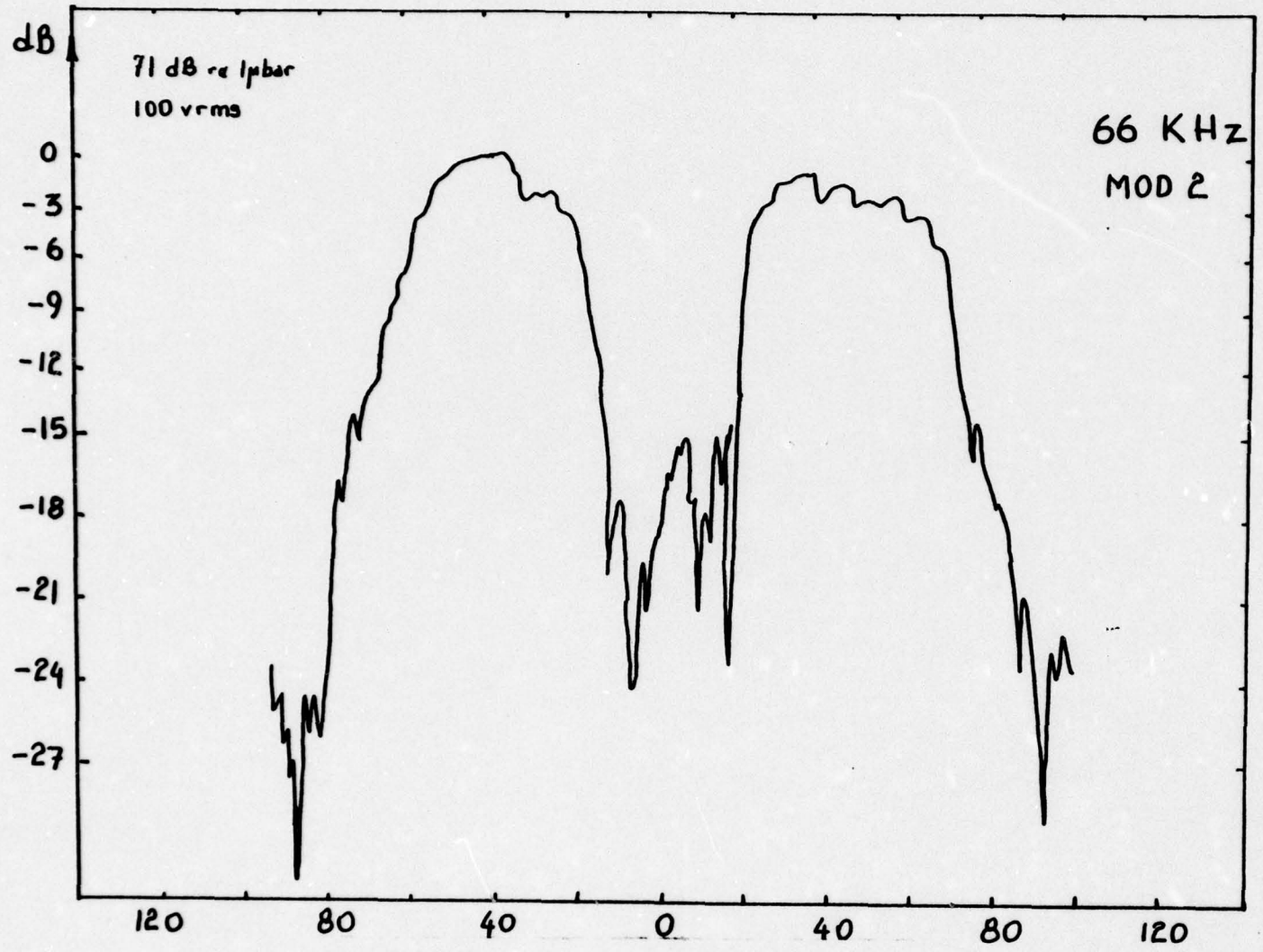

Figure 24 - RADIATION PATTERN

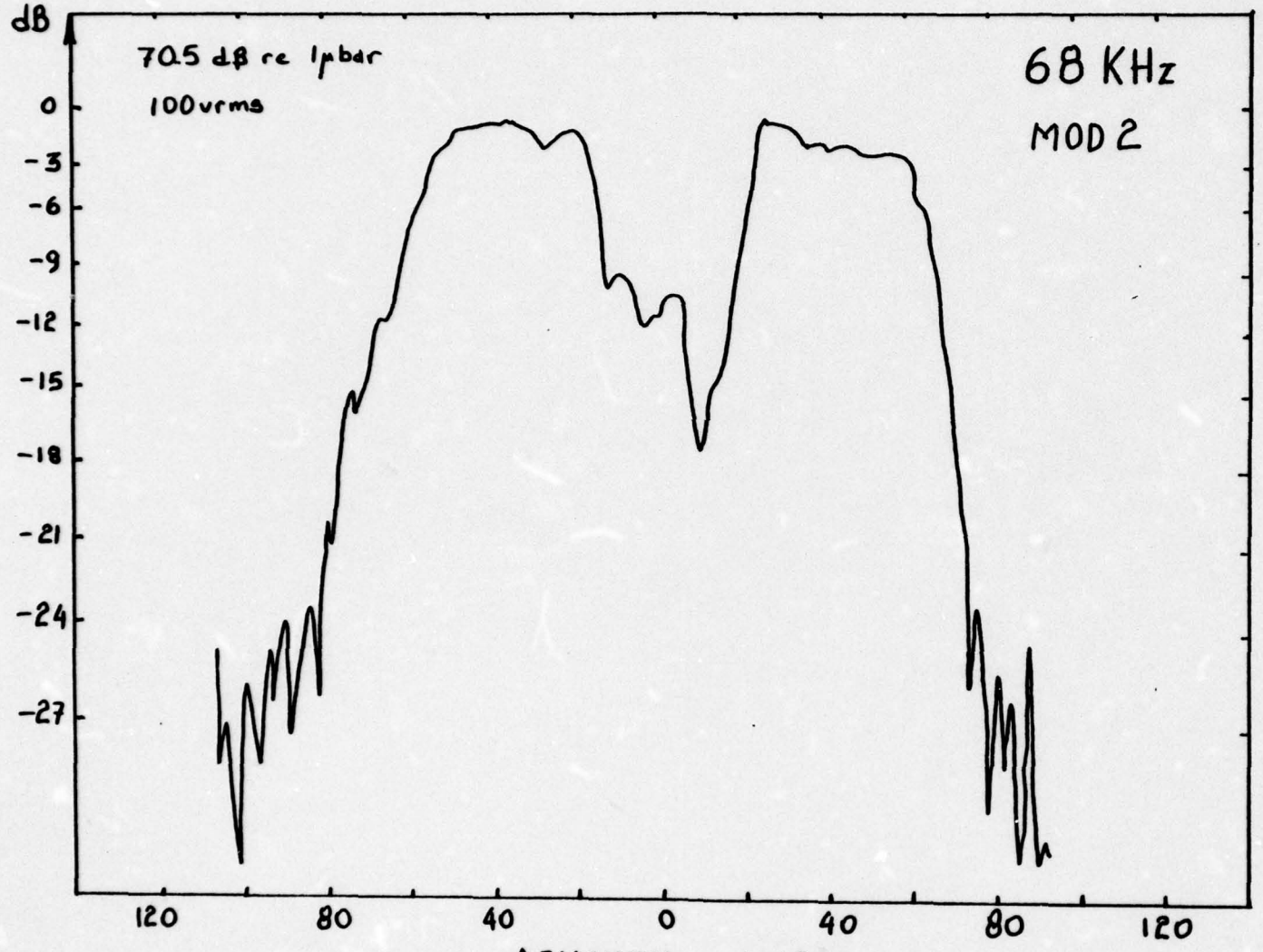

Figure 25 - RADIATION PATTERN

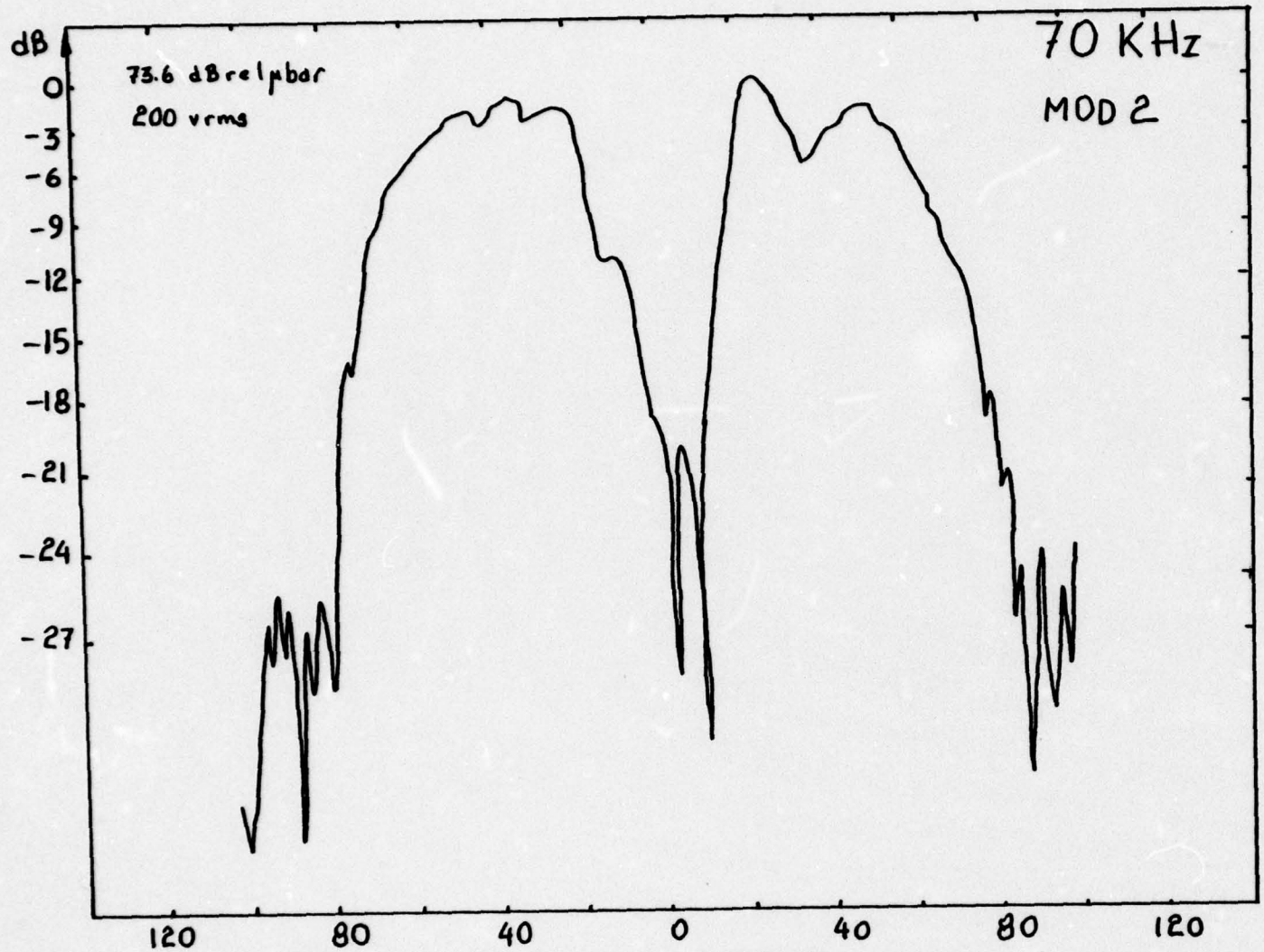

Figure 26 - RADIATION PATTERN

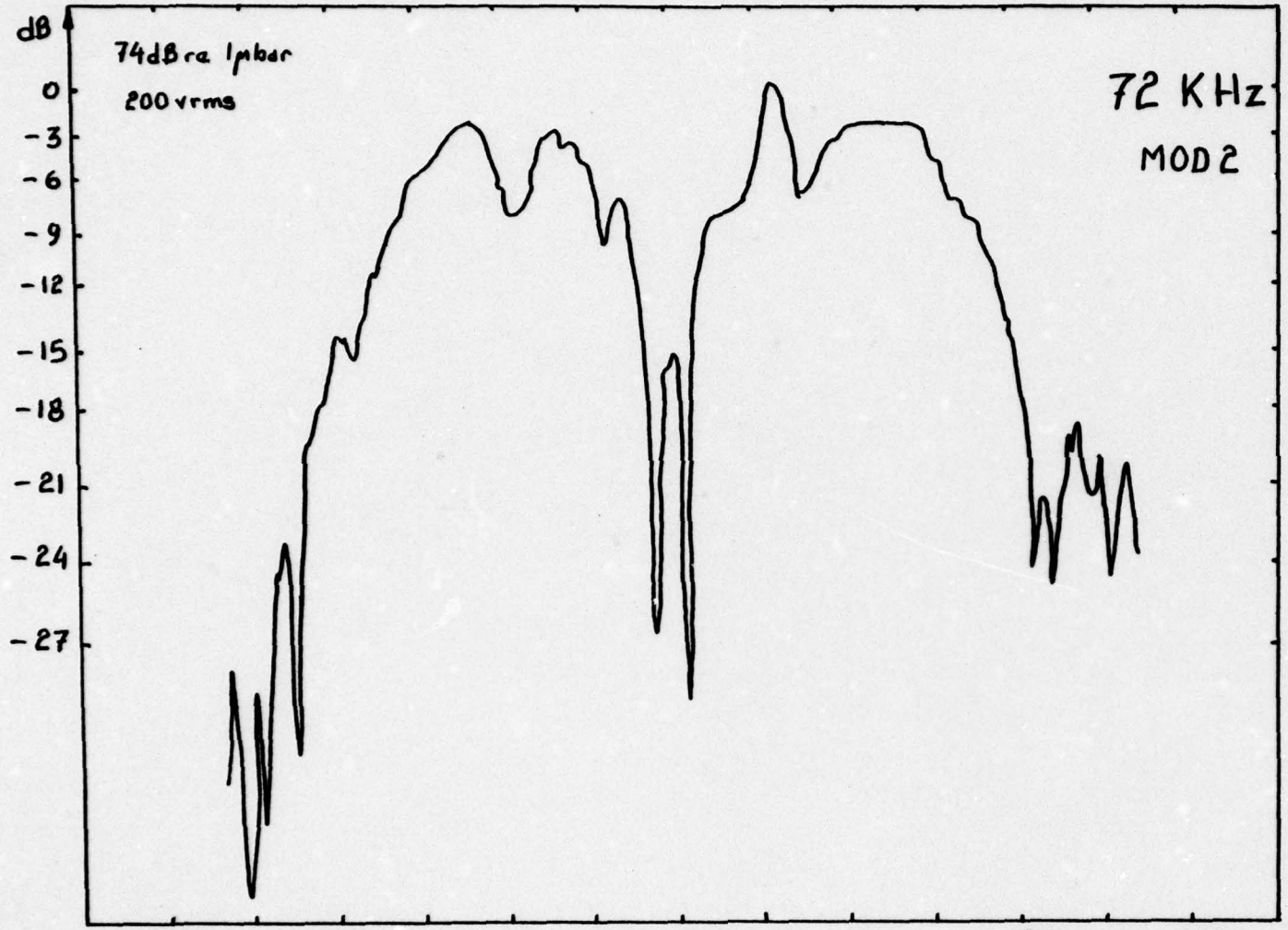

Figure 27 - RADIATION PATTERN

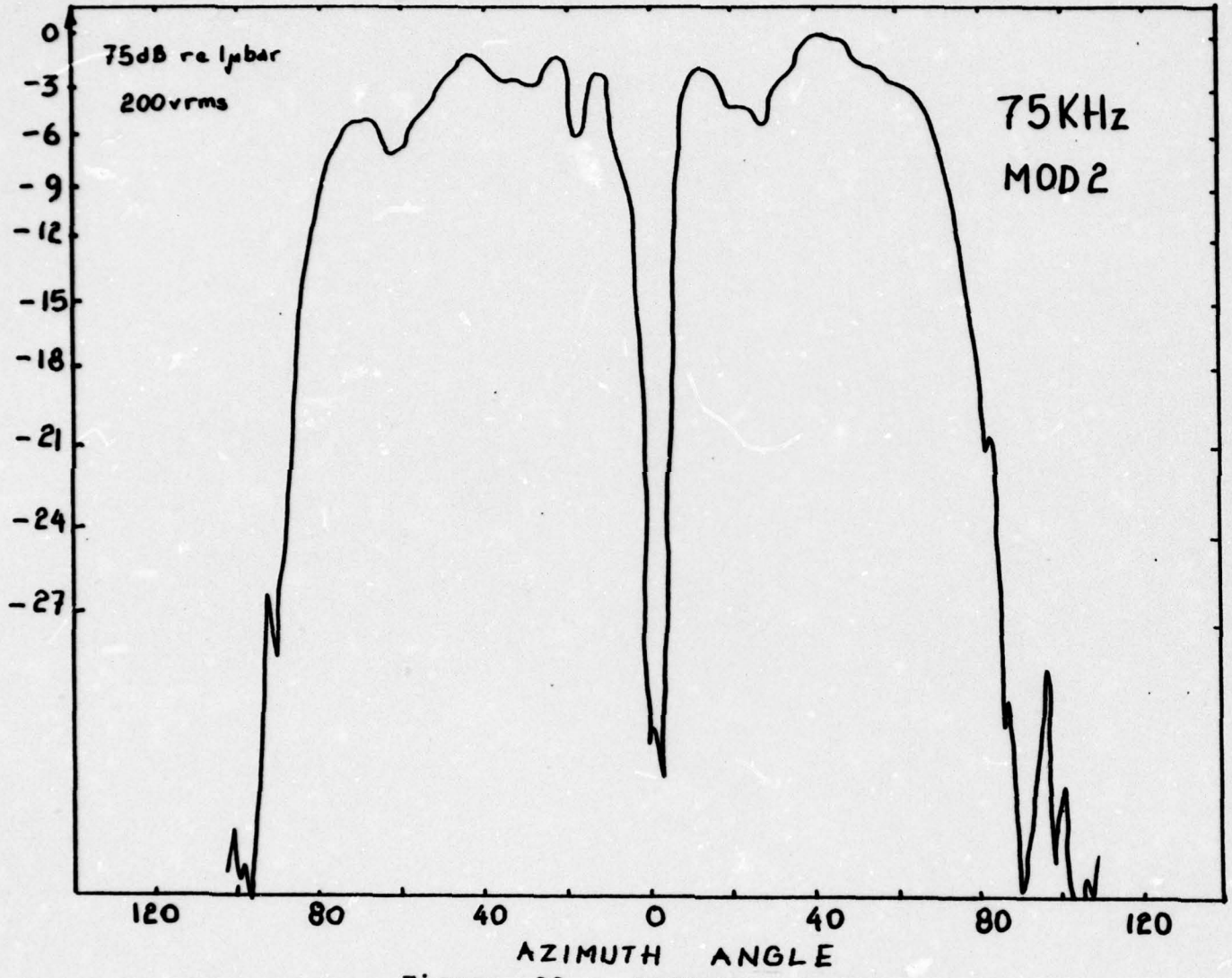

Figure 28 - RADIATION PATTERN

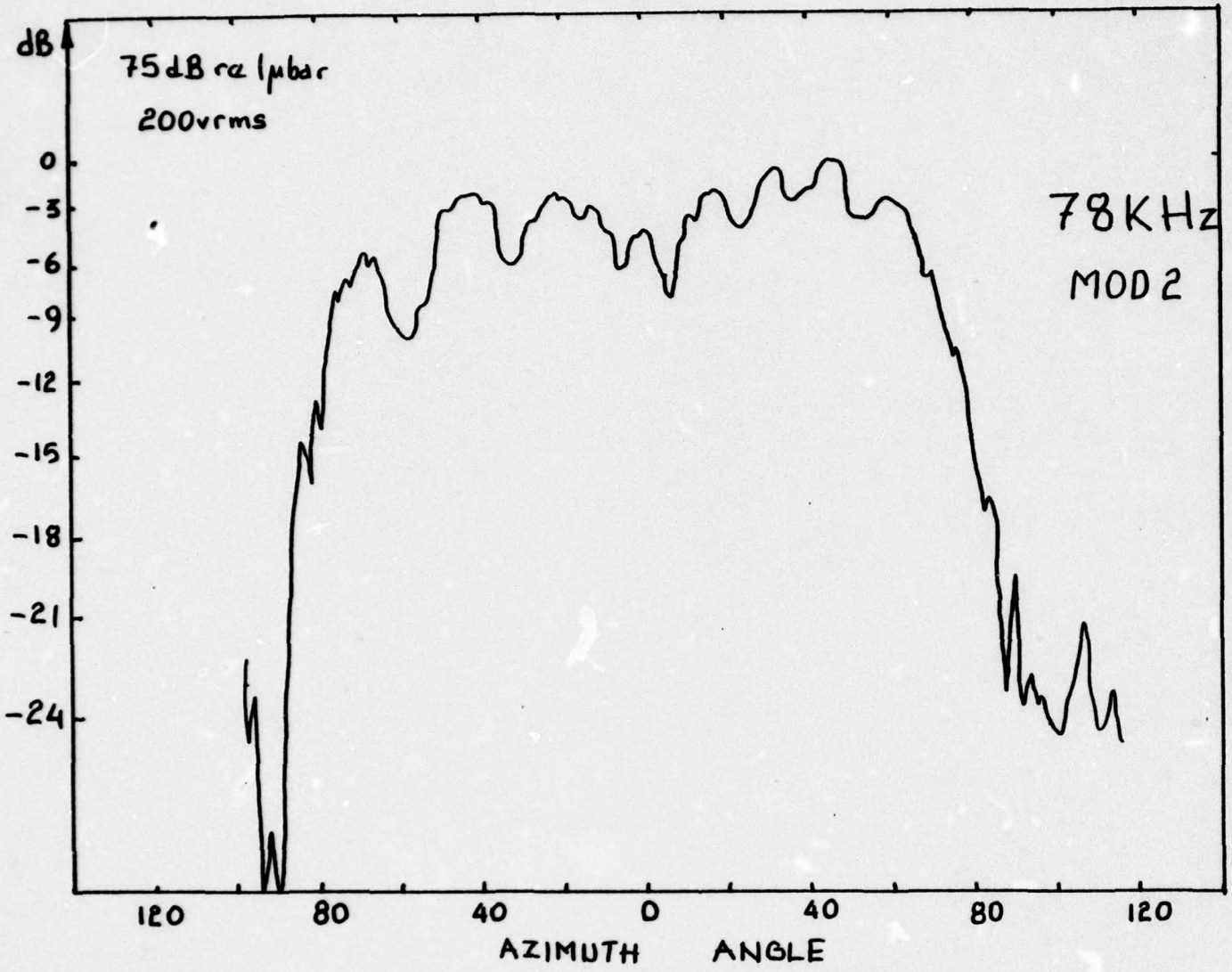

Figure 29 - RADIATION PATTERN

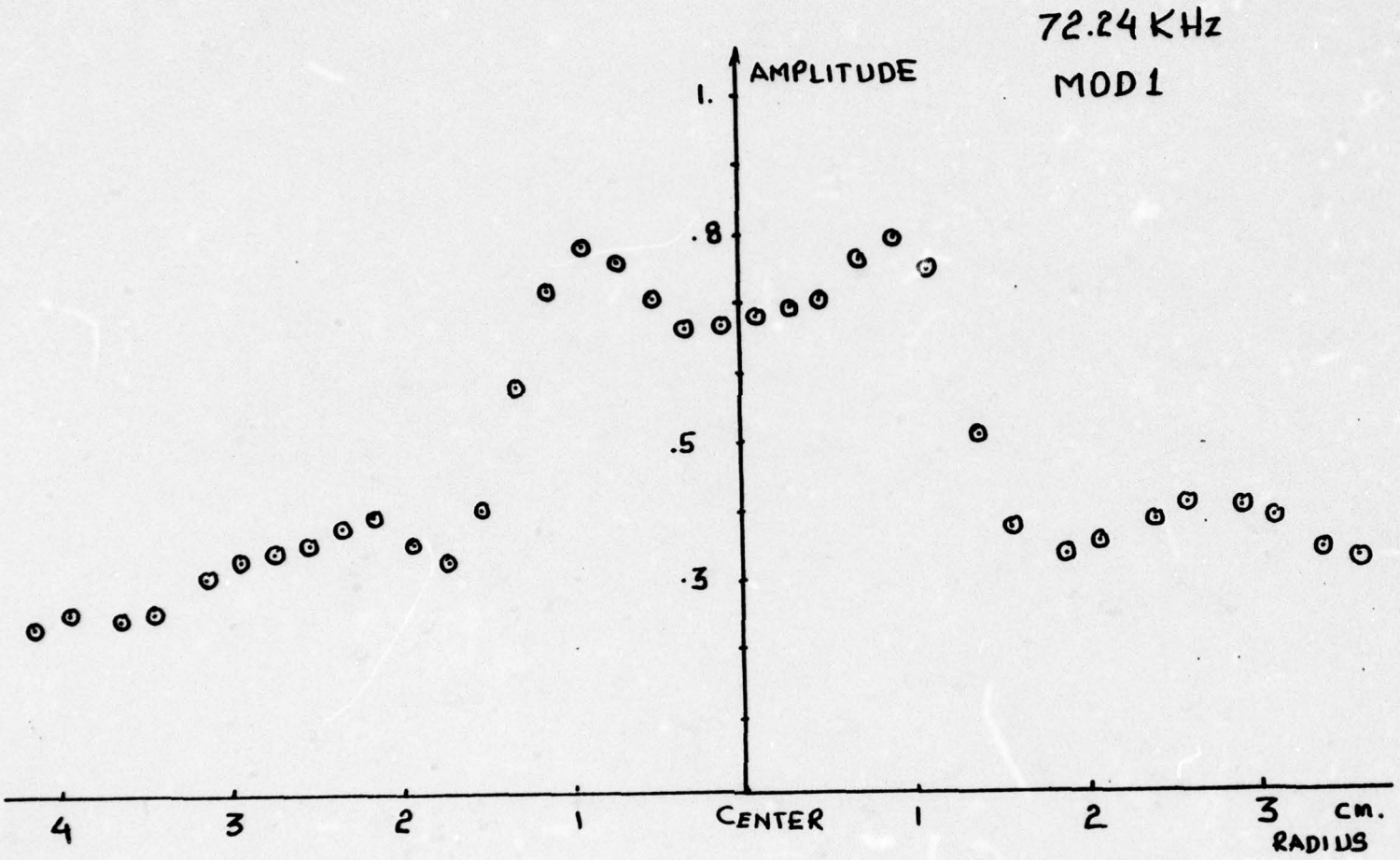

Figure 30 - NEAR FIELD PRESSURE AMPLITUDES

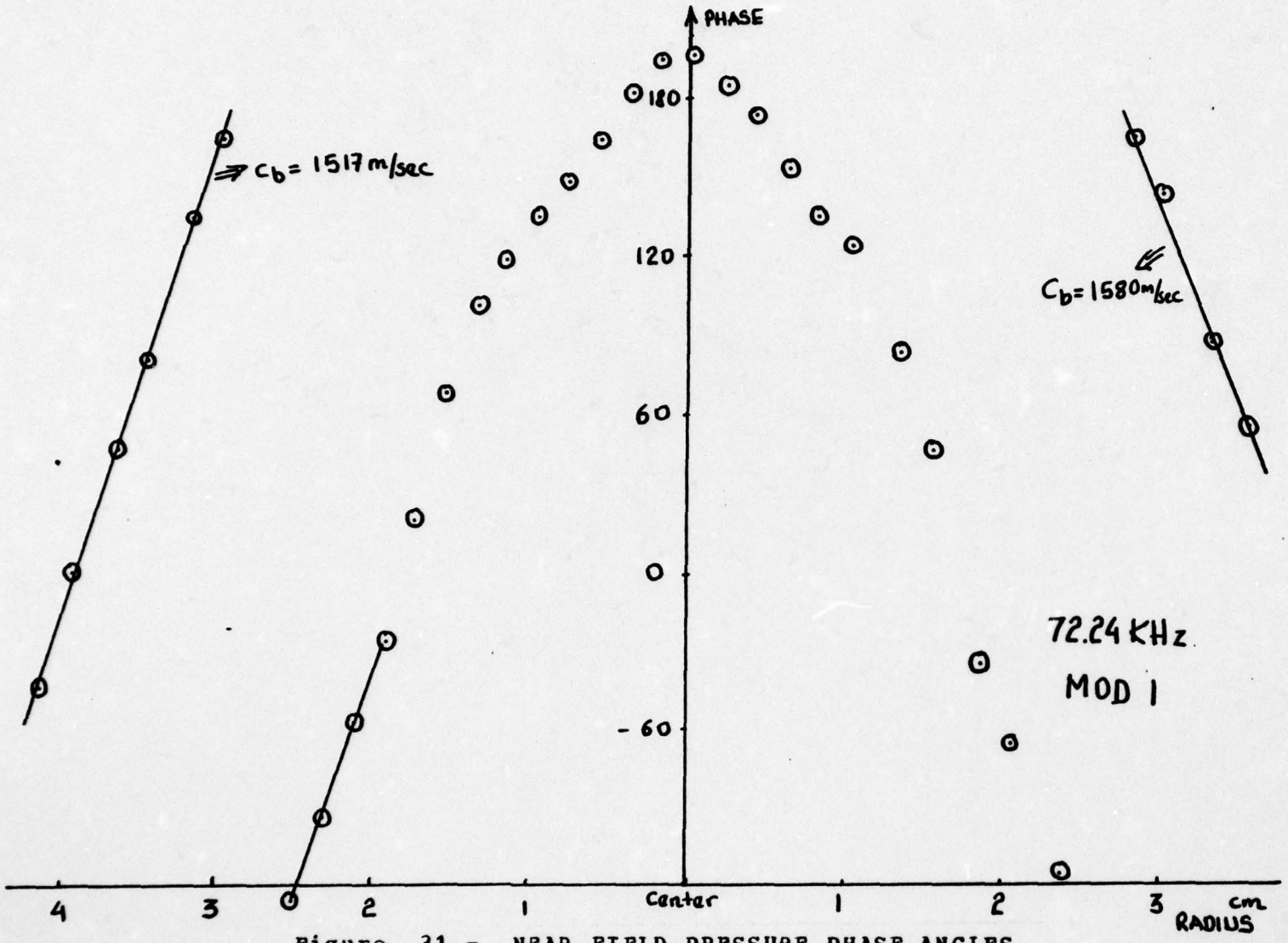

Figure 31 - NEAR FIELD PRESSURE PHASE ANGLES

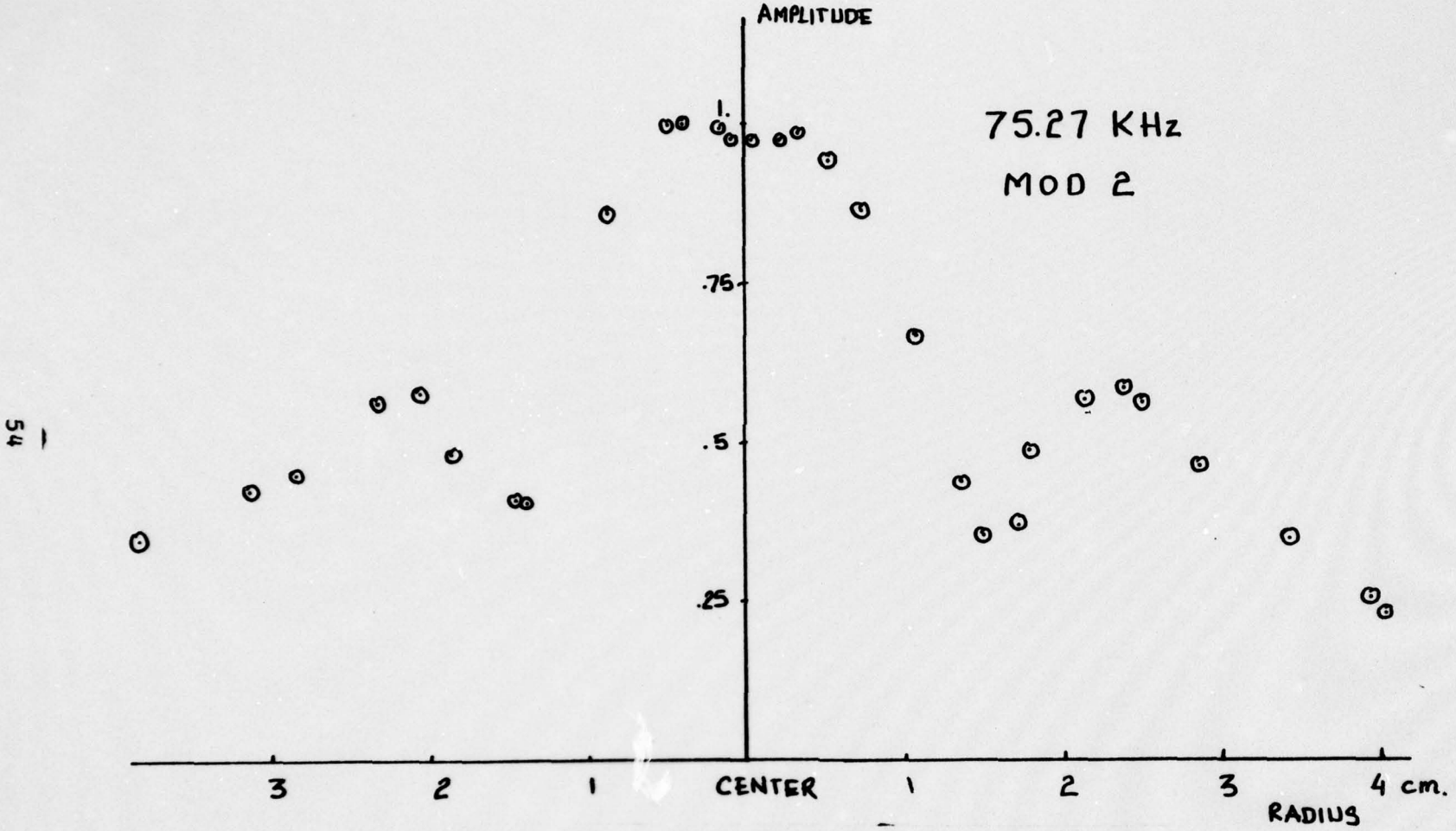

Figure 32 - NEAR FIELD PRESSURE AMPLITUDES

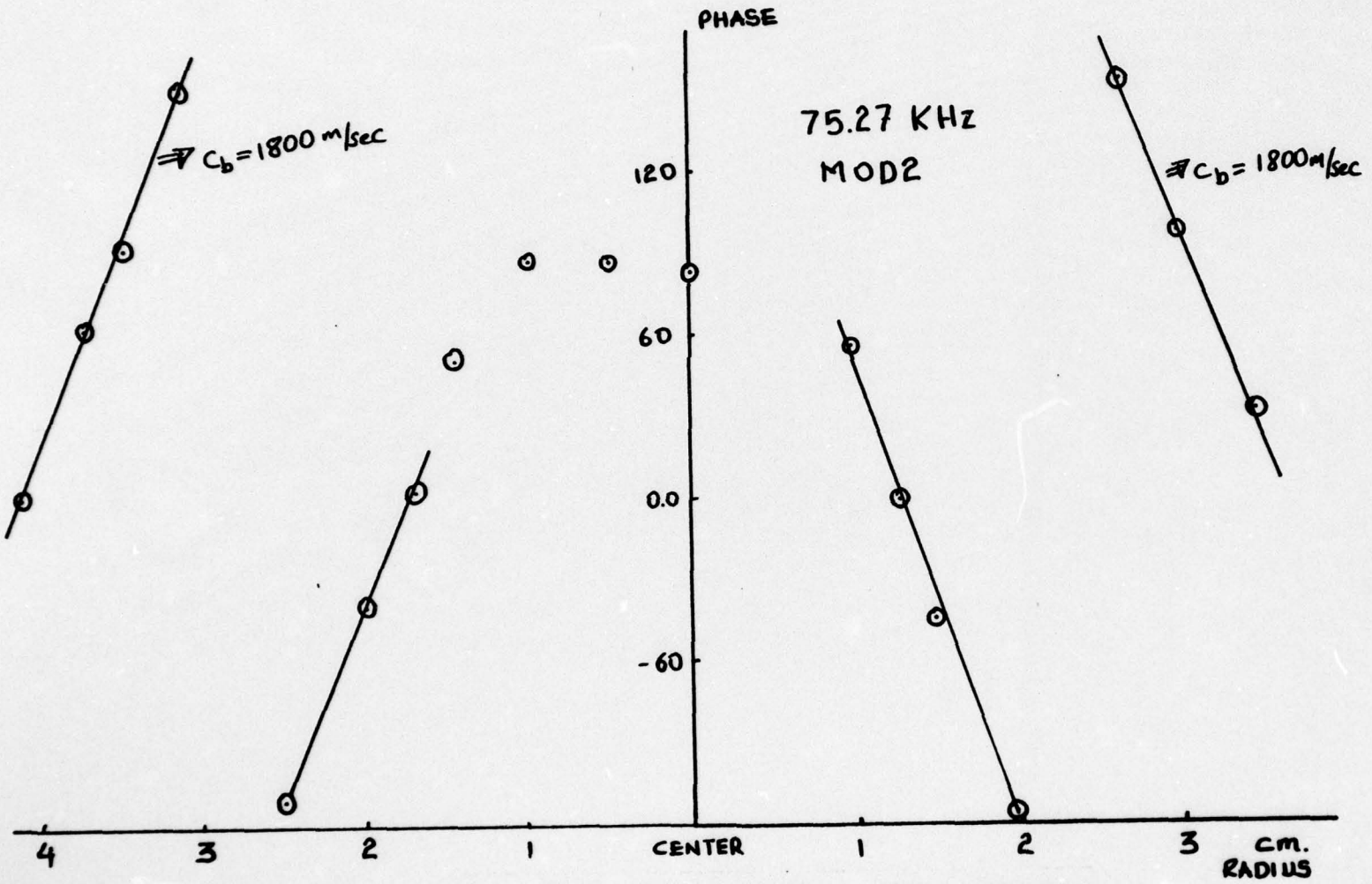

Figure 33 - NEAR FIELD PRESSURE PHASE ANGLES

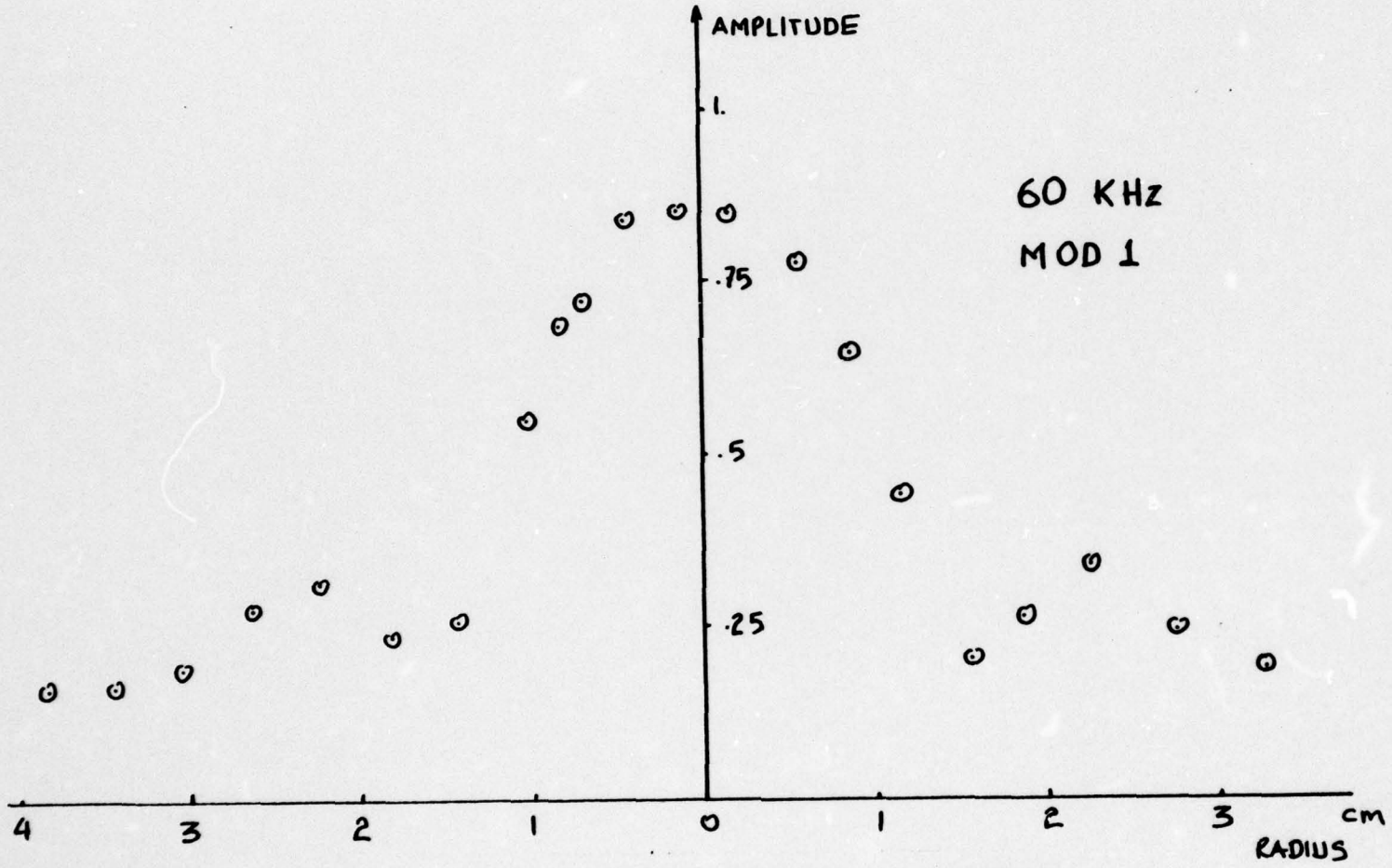

Figure 34 - NEAR FIELD PRESSURE AMPLITUDES

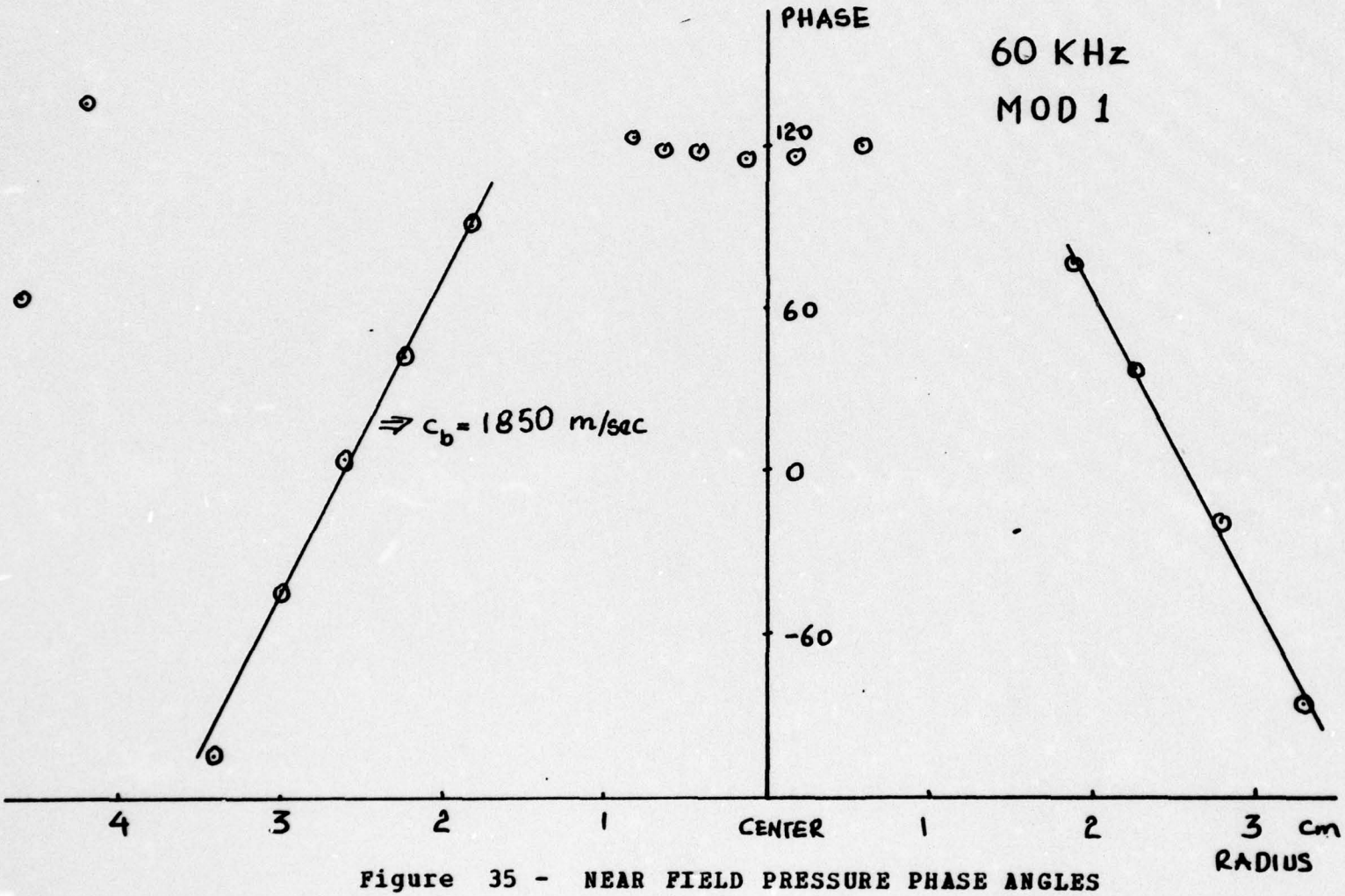

Figure 35 - NEAR FIELD PRESSURE PHASE ANGLES

IV. SUMMARY OF AND DISCUSSION OF RESULTS AND SOME CONCLUSIONS

There are some discrepancies between predicted normal mode frequencies and those actually measured which are difficult to account for quantitatively.They are most likely due to violations of the thin plate assumption and perhaps due to coupling between the modes of the plate with those of the longitudinal driver vibrator.

From the admittance curves obtained when in water , the only resonance frequencies appear to be those of the driving element.

This forces the conclusion that the radiation resistance completely damps the normal mode flexural resonances in the plate.The radiation which does occur then must be due to flexural waves propagating radially outward from the driver element located at the center of the plate.

This conclusion is also supported somewhat by the results of the near field measurements.In Figs 30,32,34, it is seen that the pressure amplitude is essentially constant over a diameter about equal to that of the driver element.Thus,the central part of the plate is behaving as a uniformly driven piston.The change in phase with radius along the plate beyond this center region corresponds to a wave speed which is higher than that in water. The phase speed of the flexural waves should increase with frequency and with plate thickness according to theory.In the three sets of data taken, the increase in phase speed with thickness was observed.The effect with frequency was

inconsistent and could not be explained.

For the reason just stated the theoretical radiation patterns calculated based on the assumption of a propagating flexural wave from a point source should not be realized,because the source is not a point.

The radiation patterns observed for the two models, shown in Figs 13-20 and Figs 24-29 can be summarized in the accompanying table(Table I).The values of the angles to the outermost -6 dB points are tabulated at various frequencies.Any dip in response along the axial direction is also noted.

There is a consistent assymmetry in the patterns which disappeared when a pattern was taken with a plane baffle.This is due to the location of the radiator nearer to one end of the cylindrical extender section used as baffle for these measurements.

The angular widths to the -6 dB points are large, varying between about 120 to 148 degrees at frequencies which cover a band width more than 6 kHz on either side of resonance.These compare favorably to the 135 degrees width specified by the Naval Torpedo Station(Ref. NAVORD 2814382 Fig 2, Modified 2-28-73, Flush 3-D Transducer Output Specifications).

The change in source level with frequency is not more than 4 dB in the band width between 60-80 kHz.

The desired dip in source level at angles near the axis is not found at all frequencies.In fact, near resonance, there appears to be a small peak near the axis.It is not possible to account for these quantitatively.The reduction found in axial source levels is probably not broad enough to

be significantly useful in reducing overall power requirements.

The maximum source level observed near resonance was about 75 dB ref. 1 microbar at 1 meter.This was for a 200 volt rms drive voltage applied,which was the maximum undistorted value available with the equipment used in these tests.From the data on the electrical admittance,the conductance at resonance is 700 micromhos.Thus at this drive voltage,the input power is about 28 watts during the pulse.

According to private communications from NTS,the desired 93 dB source level is achieved with about 400 watts input power during the pulse.It is seen that this transducer,if driven with 400 watts,and if it were linear in response,would have a maximum source level of about 87 dB,about 6 dB less than that desired.

TABLE I

FIG NO.	f kHz	OUTER -6dB ANGLES LEFT	OUTER -6dB ANGLES RIGHT	WIDTH	INNER -6dB ANGLES LEFT	INNER -6dB ANGLES RIGHT	WIDTH	MAXIMUM SOURCE LEVEL	REMARKS
			MODE I						
13	56	80	57	137	26	10	36		-15 dB
14	60	56	68	124	15	15	30	70dB 140vrms	-10 dB
15	66	80	68	148					One sharp min. not on the axis -5dB
16	70	80	60	140					Two sharp dips each side of axis
17	75	25 -12dB [82]	32 [72]	57 [154]				72dB 140vrms	Peak on axis
18	77	77	70	147					Peak along axis
19	80	78	69	147					Several dips small peak on axis
20	86	60	66	126					Essentially Flat
			MODE II						
24	66	59	70	129	18	22	40	71dB 100vrms	Dip ~ 22 dB
25	68	56	63	119	15	21	36	70.5dB 100vrms	Several dips, mostly -12dB
26	70	61	65	126	15	19	34	73.6dB 200vrms	2 sharp -30dB dips
27	72	60	66	126	15	20	35	74 dB 200vrms	2sharp -30dB dips
28	75	72	68	140	9	9	18	75dB 200vrms	One deep min. -30dB
29	78	68	68	136	-	-	-	75dB 200vrms	2or 3 dips below -6dB
			SPECIFIED						
	75	67	67	135					Minimum 93dB re 1pbar source Level is required

V. RECOMMENDATIONS

Because of the promising results mentioned above, further study is recommended.

The electromechanical efficiency can probably be improved somewhat if piezoelectric ceramic elements more suitable for this application were chosen. For example, one should use ceramic elements for the vibrator which have parallel field coupling and appropriate composition. The 33 coupling instead of the 31 coupling used here should increase the electromechanical coupling coefficient and give a larger operating band width. The ceramic composition should be one designed for high power use (The Glennite HS-21 used here is more appropriate for hydrophone use).

Some problems which must also be addressed if this approach is to be of practical use:

The obtaining of a curved face to fit the curvature of the torpedo. This could be achieved by a rubber window which has same ρc as water which is molded to the flat disk.

The radiation face of the transducer could be made larger with a possible resulting increase the source level.

Further experimental tests on the effect of plate thickness with rubber window in place are recommended. An empirical approach is necessary to determine optimum plate thickness to get the desired radiation pattern.

APPENDIX A

COMPUTER PROGRAM FOR NORMAL MODE SOLUTION

```
      DIMENSION  A(20),U(21),PTZ(20),DARG(20),X(30),Y(30),UDIF(20)
     1,FJ(20)
      R=RADIUS(M.)
      BE=2.007
      U(21)=0.
      PI=3.14159
      PK=2.*PI*75000./1500.
  100 FORMAT(4X,E12.5,10X,E12.5)
      C=PI*BE
      CALL BESJ(C,0.,DJ,.1,IER)
      DO 17 M=1,20
      ABOB=1.
      XM=M
      Z=C*XM/20.
      H=(Z/2.)**2
      DO 15 I=1,6
      ABT=1.
      DO 16 K=1,I
      FACT=ABT*K
      ABT=FACT
   16 CONTINUE
      SQF=ABT**2
      AB=H**I/SQF+ABOB
      ABOB=AB
   15 CONTINUE
      FJ(M)=ABOB
   17 CONTINUE
      EJ=FJ(20)
      DO 1 I=1,20
      YI=I
      A(I)=R/20.*YI
      PTZ(I)=A(I)**2
      B=C*YI/20.
      CALL BESJ(B,0.,DJ,.1,IER)
      U(I)=BJ-DJ*FJ(I)/EJ
      WRITE(6,100)A(I),U(I)
    1 CONTINUE
      TOT=0.
      DO 2 I=1,20
      K=K+1
      UDIF(I)=U(I)-U(K)
      AXP=PTZ(I)*UDIF(I)+TOT
      TOT=AXP
    2 CONTINUE
      PTZA=ABS(TOT)/2.
      WRITE(6,300) PTZA
  300 FORMAT(//,2X,'AXIS PRESSURE',2X,E12.5)
  500 FORMAT(//,3X,'ANGLE',10X,'PRESSURE',14X,'DECIBEL')
```

```
      WRITE(6,500)
      DO 4 I=1,30
      J=3*I
      X(I)=J
      TH=X(I)/57.29578
      ATOT=0.
      DO 5 K=1,20
      ARGO=PK*A(K)*SIN(TH)
      CALL  BESJ(ARGO,1,BJ,.1.IER)
      DARG(K)=BJ*PTZ(K)/ARGO
    5 CONTINUE
      DO 6 M=1,20
      PTI=DARG(M)*UDIF(M)+ATOT
      ATOT=PTI
    6 CONTINUE
      PDB=20.*ALOG10(ABS(PTI/PTZA))
      WRITE(6,400)J,PTI,PDB
  400 FORMAT(4X,I3,8X,E12.5,8X,F10.3)
      Y(I)=PDB
    4 CONTINUE
      CALL PLOTP(X,Y,30,0)
      STOP
      END
```

COMPUTER PROGRAM FOR PROGRESSIVE WAVE SOLUTION

```
      DIMENSION UR(20),UI(20),PTZ(20),DARG(20),X(30),Y(30),Z(30),
     1URDIF(20),UIDIF(20),A(20)
  100 FORMAT(4X,E12.5,10X,E12.5)
  200 FORMAT(4X,'TOTR=',E12.5,10X,'TOTI=',E12.5)
  300 FORMAT(5X,'PTZAM=',E12.5,'FIAX=',F5.2)
  400 FORMAT(4X,I3,10X,E12.5,10X,F5.2)
  500 FORMAT(//,3X,'ANGLE',10X,'PTOTM' ,14X,'FTOT')
      H=HALF THICKNESS (M.)
      R=RAIUS (M.)
      UR(21)=0.
      UI(21)=0.
      PI=3.14159
      PK=2.*PI*75000./1500.
      WM=12.257/H**.5
      WK=WM*R
      DO 1 I=1,20
      RK=WK*I/20.
      CALL BESJ(RK,0,BJ,.1,IER)
      CALL BESY(RK,0,BY,IEB)
      A(I)=R/20.*I
      PTZ(I)=A(I)**2
      WRITE(6,100)BY,BJ
      UR(I)=BY
      UI(I)=BJ
    1 CONTINUE
C     CALC  AXIS  PRESSURE
      TOTR=0.
      TOTI=0.
      DO 2  I=1,20
      K=I+1
      URDIF(I)=UR(I)-UR(K)
      UIDIF(I)=UI(I)-UI(K)
      AXPR=PTZ(I)*URDIF(I)+TOTR
      AXPI=PTZ(I)*UIDIF(I)+TOTI
      TOTR=AXPR
      TOTI=AXPI
      WRITE(6,200)TOTR,TOTI
    2 CONTINUE
      PTZAM=ABS((TOTR*TOTR+TOTI*TOTI)**.5)/2.
      FIAX=ATAN(TOTI/TOTR)
      WRITE(6,300)PTZAM,FIAX
      WRITE(6,500)
C     CALC  PRESSURE  FROM  AXIS
      DO 4    I=1,30
      J=3*I
      X(I)=J
      TH=X(I)/57.29578
      ATOT=0.
```

```
      BTOT=0.
      DO   5   K=1,20
      ARGO=PK*A(K)*SIN(TH)
      CALL   BESJ(ARGO,1,BJ,.1,IER)
      DARG(K)=BJ*PTZ(K)/ARGO
    5 CONTINUE
      DO 6   M=1,20
      PTIR=DARG(M)*URDIF(M)+ATOT
      PTII=DARG(M)*UIDIF(M)+BTOT
      ATOT=PTIR
      BTOT=PTII
    6 CONTINUE
      PTOTM=(ATOT*ATOT+BTOT*BTOT)**.5
      FTOT=ATAN(BTOT/ATOT)
      PDB=20.*ALOG10(ABS(PTOTM/PTZAM))
      FREL=FTOT-FIAX
      Y(I)=PDB
      Z(I)=FREL
      WRITE(6,400)J,PTOTM,FTOT
    4 CONTINUE
      CALL  PLOTP(X,Y,30,0)
      CALL  PLOTP(X,Z,30,0)
      STOP
      END
```

LIST OF REFERENCES

1. Morse and Ingard, Theoretical Acoustics, p. 213 to 217, Mc Graw Hill, 1968.

2. Malecki, Physical Foundations of Technical Acoustics, p. 505 to 523, Pergamon Press, 1969.

3. Kinsler and Frey, Fundamentals of Acoustics, p. 502, John Wiley and Sons, 1962.

4. Shaw,A.H.P.,Radiation Pattern of a Two-Element,Concentric Ring Transducer Using Phase and Amplitude,Shading,M.Sc. Thesis,Naval Postgraduate School,1975

INITIAL DISTRIBUTION LIST

		No. Copies
1.	Deniz K. Komutanligi Bakanliklar-Ankara,TURKEY	1
2.	Library,Code 0212 Naval Postgraduate School Monterey,California 93940	2
3.	Department Chairman Code 61 Department of Physics and Chemistry Naval Postgraduate School Monterey,California 93940	1
4.	Professor O. B. Wilson,Code 61 Wl Department of Physics and Chemistry Naval Postgraduate School Monterey,California 93940	5
5.	Department Library,Code 61 Department of Physics and Chemistry Naval Postgraduate School Monterey,California 93940	1
6.	Middle East Technical University Library Ankara,TURKEY	1
7.	Istanbul Teknik Universitesi Kutuphanesi Taskisla-Istanbul,TURKEY	1

8. Deniz Harbokulu Komutanligi 1
Kutuphanesi
Heybeliada-Istanbul,TURKEY

9. Mr.R.L.Marimon,Code 7000 2
Naval Torpedo Station
Keyport,Washington 98345

10. Mr.Michael L. Barlow,Code 7042 1
Naval Torpedo Station
Keyport,Washington 98345

11. Lt. Omer SEVDIK 2
Atakoy 3.Kisim No:52-3
Istanbul,TURKEY

12. Defense Documentation Center 2
Cameron Station
Alexandria, Virginia 22314